

FBSDetector: Fake Base Station and Multi Step Attack Detection in Cellular Networks using Machine Learning

Kazi Samin Mubasshir*
Purdue University
West Lafayette, IN, USA
kmubassh@purdue.edu

Imtiaz Karim*
Purdue University
West Lafayette, IN, USA
karim7@purdue.edu

Elisa Bertino
Purdue University
West Lafayette, IN, USA
bertino@purdue.edu

ABSTRACT

Fake base stations (FBSes) pose a significant security threat by impersonating legitimate base stations. Though efforts have been made to defeat this threat, up to this day, the presence of FBSes and the multi-step attacks (MSAs) stemming from them can lead to unauthorized surveillance, interception of sensitive information, and disruption of network services for legitimate users. Therefore, detecting these malicious entities is crucial to ensure the security and reliability of cellular networks. Traditional detection methods often rely on additional hardware, predefined rules, signal scanning, changing protocol specifications, or cryptographic mechanisms that have limitations and incur huge infrastructure costs in accurately identifying FBSes. In this paper, we develop FBSDetector—an effective and efficient detection solution that can reliably detect FBSes and MSAs from layer-3 network traces using machine learning (ML) at the user equipment (UE) side. To develop FBSDetector, we created FBSAD and MSAD, the *first-ever* high-quality and large-scale datasets for training machine learning models capable of detecting FBSes and MSAs. These datasets capture the network traces in different real-world cellular network scenarios (including mobility and different attacker capabilities) incorporating legitimate base stations and FBSes. The combined network trace has a volume of 6.6 GB containing 751963 packets. Our novel ML models, specially designed to detect FBSes and MSAs, can effectively detect FBSes with an accuracy of 92% and a false positive rate of 5.96% and recognize MSAs with an accuracy of 86% and a false positive rate of 7.82%. We deploy FBSDetector as a real-world solution to protect end-users through an Android app and validate in a controlled lab environment. Compared to the existing heuristic-based solutions that fail to detect FBSes, FBSDetector can detect FBSes in real time.

1 INTRODUCTION

The widespread adoption of cellular networks has brought about unprecedented improvements in data rates, latency, and device connectivity, resulting in a surge in the number of connected devices worldwide. In 2023, the number of mobile devices is assessed at 16.8 billion having an estimated 5.25 billion global users, marking a 4.9% annual increase [1], and the number of mobile devices is expected to reach 18.22 billion by 2025 having 5.67 billion users [2]. Given the extensive usage and dependence on cellular networks, they become desirable targets for malicious entities. These entities try to disrupt cellular network services by exploiting different types of vulnerabilities in cellular network protocols with the help of sophisticated hardware. Of all the attacks and threat models targeting cellular

networks, Fake Base Stations (FBSes), a.k.a. rouge base stations, stingrays, and IMSI catchers, are among the most widespread and represent a significant threat. Due to the lack of authentication of initial broadcast messages as well as the unprotected connection setup in the bootstrapping phase [3,4], adversaries can install FBSes that can lure unsuspecting devices to connect to them and then launch sophisticated multi-step attacks (MSAs) [5–11].

Motivation. The threat posed by FBSes is not new and has been around for a while, but they are still extensively used by attackers worldwide [12, 13]. The key motivations of our work are: (1) *A persistent problem.* Despite numerous efforts, FBSes are still one of the most persistent problems in cellular network security and can be deployed and used for attacks in 5G cellular networks, despite the use of the encrypted permanent ID SUCI compared to the unencrypted IMSI in 4G, which the UE sends to the base station for authentication [14]. Recent efforts have introduced certificate-based solutions and digital signatures [15–17] to address such problems. Nonetheless, these proposals are still in their infancy and would impose substantial overhead and require changes to the specifications to be applicable in a real-world setting. Moreover, the proposed certificate-based solutions make the design of roaming difficult for cellular network providers. When a user travels from one place to another place or from one country to another country, the different network providers will have to share their secret keys for authentication, which is very challenging considering the security aspects of the sharing process [18]. (2) *Billions of unprotected devices.* The 3GPP is planning to incorporate several defense mechanisms in the protocol to defend against FBSes [17] in future generations. However, these defense mechanisms will still take several years to roll out in the specification and then to the implementation. Currently, billions of devices worldwide are vulnerable to FBS-based attacks, and billions of new devices released in the coming years will be vulnerable to attacks until the new protocol is implemented. These devices need to be secured through in-device solutions because replacing them is impractical and would incur huge costs. (3) *Impracticality and high cost of existing defense mechanisms.* Although efforts [3, 4, 19–33] have been undertaken to detect and take down FBSes, they suffer from at least one of the following limitations: (A) Heuristic [30, 31, 33] and signature [3] based solutions fail to adapt to the detection of ever-evolving attacks. (B) Some solutions depend on crowd-sourced data [29], which is impractical to scale up to a system that has to protect billions of devices. (C) Some detection solutions [21–23, 34, 35] require installing expensive hardware; in most cases, they are proprietary. For example, CellDAM [36] requires a separate companion node near the UEs to capture the signaling messages. This is not a practical solution for protecting billions of devices. (D) Lower layer based solutions [19, 20, 24–28, 37]

*Equal contribution. The student author’s name is given first.

cannot detect sophisticated FBSes, and are not inherently able to detect MSAs.

Recently, both Google and Apple have taken new ways to defeat FBSes [38]. Though promising, these measures have little impact on a knowledgeable and well-equipped adversary. Therefore, it is essential to design effective and efficient solutions able to detect FBSes and MSAs. In this paper, we aim to address such a need by developing a low-overhead, no-cost, and in-device solution that can effectively detect FBSes and MSAs that use FBSes in their threat model, from the network traces in the UEs.

A practical solution. Machine learning (ML) can be a practical in-device solution to address all the existing problems in detecting and defending against the FBSes and MSAs. On a high level, an ML-based solution has the following benefits: ❶ It can protect all the existing end-user devices vulnerable to the attacks. ❷ No change is required in the protocol. Using the network traces, especially the higher layer (layer 3) traces, the ML algorithms can determine if there are any FBSes in the network and recognize MSAs. ❸ No additional hardware is required. ❹ ML algorithms add little overhead regarding memory and power consumption. ❺ As the attack patterns are similar worldwide, ML algorithms can detect FBSes and MSAs anywhere in the world and thus can support roaming of the device they are deployed in.

A critical issue when applying ML techniques to FBS and MSA detection is which features to use. Most previous solutions rely on features extracted from the physical layer traces. However, as mentioned earlier, such approaches have several limitations. Our insight about this issue is that features extracted from traces at the layer-3 protocols are much more informative - which is critical for being able to detect not only FBSes but also detect and classify MSAs, especially when dealing with sophisticated attackers.

Challenges. The design of an ML-based system for the detection of FBSes, however, requires addressing several major challenges: (1) Acquiring a comprehensive and high-quality dataset encompassing a wide range of real-world cellular network scenarios. (2) Incorporating the surrounding context into consideration. Unlike traditional methods where packets can be inherently malicious, in this problem, the true nature of a packet hinges on “when” and “in which context” it was sent. (3) Capturing, representing, and learning the unique characteristics that define these MSAs. The actual challenge lies in learning these complex attack signatures. This task requires the deployment of sophisticated ML algorithms that not only recognize known attack patterns but also adapt to evolving attacks. (4) Combining the predictions of layer-3 protocols. Layer-3, also known as the network layer, has two key protocols: (1) NAS (Non-Access Stratum) [39] and (2) RRC (Radio Resource Control) [40]. These protocols operate within the control plane, each serving distinct purposes in facilitating communication between User Equipment (UE) and the network infrastructure. To have a unified detection and improve robustness, the predictions made separately for the two protocols need to be combined. (5) Enabling real-time detection of the attacks. The framework needs to be an in-device solution that captures, processes and analyzes incoming packets promptly to detect the presence of the attacks effectively.

Our approach. To detect FBSes effectively, in this paper, we present the design, implementation, and deployment of FBSDetector, an ML-based framework for FBS detection and MSA recognition. As it

is illegal to create FBSes in public areas and there are no publicly available datasets of FBS and MSA traces, we create FBSAD and MSAD, the first comprehensive and high-quality FBS and MSA datasets, respectively. To achieve this, we utilize different facilities at POWDER [41]. POWDER is a city-scale and end-to-end software-defined platform to support mobile and wireless research. The dataset created using POWDER is analogous to real-world datasets. This is ensured by including over-the-air actual packets transmitted within its spectrum between actual devices instead of simulated wire transmissions [42–46]. FBSAD and MSAD incorporate different networking scenarios (static and mobile endpoints) and different attacker capabilities (from less sophisticated to more sophisticated). To tackle the second challenge, that is, incorporating the surrounding context into detection, we design a Sequential-LSTM model that takes sequence length as a hyperparameter and trains on chunks of packets. This ensues from our intuition that the length of the sequence of FBS-generated messages follows a specific distribution (see Section 6.1). For MSA detection, we use graph learning–derived from our intuition that all the MSAs follow a specific pattern (see Section 4.2.2), and that to recognize an MSA successfully, it is necessary to capture these patterns. We construct a directed graph from the packets to capture the patterns and train a graph learning model on these graphs to learn the patterns. Moreover, through using maximum overlapping sub-graphs, we can detect unseen attacks and recognize the MSAs, even if they evolve or the attackers try to evade detection by re-shaping traffic (see Section 4.2.2). To obtain a unified prediction we combine predictions made on NAS and RRC packets using a weighted confidence-based fusion method. This method of combining predictions enhances detection accuracy beyond individual predictions. For the deployment of FBSDetector, we create a mobile app that can scan the network and analyze the packet traces by running the pre-trained models on the device to detect FBSes and MSAs effectively in real time.

Experimental results. The unprocessed FBSAD and MSAD datasets have a combined size of 6.6 GB. After the initial filtering, we have 751963 packets in total. Trained on this combined dataset, our experiments show that our Sequential-LSTM model can detect FBS with 92% accuracy and a false positive rate of 5.96%. Similarly, our graph learning model can detect 9 MSAs with 86% accuracy and a false positive rate of 7.82%. Our experiments also show that combining NAS and RRC predictions using weighted confidence-based fusion method improves the performance beyond the individual models trained on NAS and RRC layers separately by 1 ~ 2%. To validate FBSDetector’s fidelity and evaluate its performance, memory and power consumption in real-world scenarios, we instantiate an Android application for 4G UEs and set up FBSes and MSAs in a controlled lab environment. Using our lab setup, we spawn an FBS and run experiments with different FBS detection and MSA recognition scenarios. The experimental results show that FBSDetector can detect FBSes in all the tested scenarios using an average 835 KB of memory and less than 2 mW of power.

Contributions. This paper makes the following contributions:

- We develop a new framework–FBSDetector to detect FBSes and MSAs from network traces using ML. For this, we create FBSAD and MSAD, the *first-ever* large-scale, high-quality, real-world datasets containing FBS and MSA traces in different scenarios.

- We design a Sequential-LSTM model for the FBS detection task, which improves the detection accuracy and lowers the false positive rates than other state-of-the-art models. For MSAs, we innovate by converting the attack signatures to graphs and using a graph-based learning approach to detect the attacks. Graph learning models perform better than any other state-of-the-art model in recognizing MSAs. Moreover, the MSAs, even if they evolve, and unseen and reshaped attacks can be detected in this approach by using maximum overlapping sub-graphs.
- We deploy the solution in an Android app and validate its performance in real environments by creating a testbed in our controlled lab setup. Compared to the available end-user FBS detection solutions, which fail to detect FBSes and MSAs, our approach effectively detects FBSes and MSAs in all the tested real-world scenarios.

Open-source. We will open-source the datasets, our models, and the Android app for further research and help end-users protect themselves from FBS-related attacks.

2 BACKGROUND

In this section, we introduce relevant background about 4G, FBSes, MSAs and POWDER—the platform we use for dataset generation.

2.1 4G Cellular Networks

In a 4G network, cellular devices are called User Equipments (**UE**). The core network is called the Evolved Packet Core (**EPC**). Geographic locations are partitioned into hexagonal cell areas, each of which is serviced by a designated base station (**eNodeB**), which enables connectivity of UEs in that cell to the EPC. The Mobility Management Entity (**MME**) manages the connectivity and mobility of UEs in a particular tracking area (a set of cell areas).

Non-Access Stratum (NAS). In 4G, the Non-Access Stratum (NAS) [39] protocol is a layer-3 (Network Layer) protocol specified by 3GPP that serves as a functional layer between the core network and the UEs. Its primary role is to manage the communication sessions and seamlessly maintain the connections with the UE, even when the UE roams.

Radio Resource Control (RRC). The Radio Resource Control (RRC) [40] protocol is another layer-3 protocol used between the UEs and the base stations. The major functions of the RRC protocol include connection establishment and release functions, broadcast of system information, radio bearer establishment, reconfiguration and release, and paging notification and release.

2.2 Fake Base Station and Multi-Step Attacks

A Fake Base Station (FBS) is an unauthorized device that impersonates a legitimate base station within a cellular network (shown in Figure 1.b). FBSes typically consist of a radio transceiver capable of broadcasting signals on the same frequencies legitimate base stations use. By emitting these signals, an FBS creates a cell or coverage area, attracting nearby mobile devices to connect to it.

When a mobile device connects to an FBS, it establishes a communication link with the FBS instead of the legitimate network. This enables the attacker operating the FBS to carry out various malicious activities, including call interception, SMS interception,

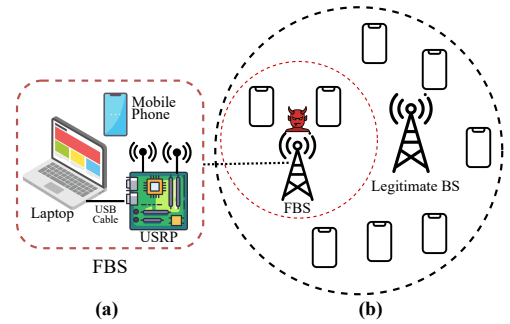


Figure 1: Operating principles of a typical FBS. Compared to a legitimate base station, an FBS usually possesses a smaller signal coverage area but a higher signal strength.

location tracking, man-in-the-middle attacks, and denial of service [6–11, 47]. Some FBSes can mimic the network name (SSID) and encryption protocols used by legitimate networks, making it difficult for users to differentiate between fake and genuine networks. This can trick users into unknowingly connecting to the FBS, making them susceptible to attacks. The system architecture of FBSes has evolved over several generations, where each generation uses different hardware and communication processes. Utilizing a FBS as a foothold, an attacker can also carry out several coordinated steps to achieve a malicious objective. These Multi-Step Attacks (MSAs) can compromise cellular communication’s integrity [5, 6], privacy [7–10], and availability [7–9, 11] and usually take several specific well-defined attack steps.

Hardware and Software. A FBS is generally made up of two components: (1) a wireless transceiver and (2) a computing unit (shown in Figure 1.a). The components are portable and require a relatively small amount of electrical power, making it easy to accommodate them in a van, a minibus, the trunk of a car, or even a backpack. The mobility of modern FBSes makes it difficult to localize and take them down. The wireless transceiver is the core component of an FBS. It can simulate most of the base-station-to-cellphone functions (i.e., it cannot forward voice, SMS, and data packets to a mobile carrier’s network) due to the absence of network authorization and the presence of security mechanisms. The computing unit, in most cases a laptop (in more modern cases a Raspberry Pi, or an Intel NUC), is usually connected to the wireless transceiver via a USB cable, through which it controls the transceiver, e.g., tuning the radio frequency, adjusting the signal strength, setting the base station ID, and other parameters. A cellphone searches for nearby, legitimate base stations and records their wireless parameters. Based on this information, the attacker can reconfigure the parameters of the FBS to mimic legitimate base stations to maximize the number of affected users.

Communication Process. To interrupt the existing connections between nearby user devices and legitimate base stations, the attacker would adjust the signal strength of the FBS to guarantee that it offers a much higher signal strength than the legitimate base station. Once the operator has properly configured the FBS, usually the following sequence of events begins to occur, culminating in

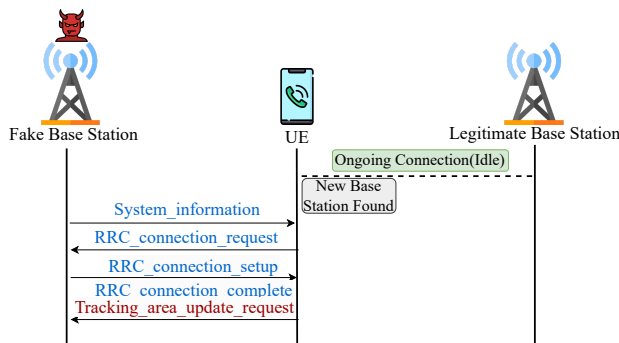


Figure 2: Usual communication process of FBSes

messages being sent to all users nearby: ① The FBS broadcasts its *system information* using the configured radio frequency. ② When a UE receives the system information of the FBS, it detects it as a new base station with a higher signal strength and sends a *tracking area update request* to the FBS. In other cases, the FBS can send a *paging request* to trigger the service procedure to establish the communication. ③ Upon receiving the *tracking area update request*, the FBS first usually sends an *identity request* to the UE to acquire its IMSI information and then sends another *identity request* to acquire its IMEI information. ④ Subsequently, the FBS sends different messages to the UE. This action can be repeated multiple times. ⑤ When the FBS completes sending messages, it cuts off the cellular connections with its UEs by lowering its signal strength or shutting down the signal. After that, the affected UEs may or may not automatically re-connect to a legitimate BS (some UE's require manual restarting to connect back). A simplified diagram of this communication process is shown in Figure 2.

2.3 POWDER

POWDER (Platform for Open Wireless Data-driven Experimental Research) [41] is a cityscale, remotely accessible, end-to-end software-defined platform funded by NSF to support mobile and wireless research and provides advances in scale, realism, diversity, flexibility, and access.

Fidelity of POWDER to the real-world. POWDER's fidelity extends beyond conventional simulation due to the following reasons: (1) POWDER provides a dedicated frequency band and real devices [41]. This access to real devices while maintaining scalability and mobility makes POWDER equivalent to real-world testbeds. (2) POWDER's fidelity is proven through rigorous testing and evaluation, demonstrating that solutions developed using POWDER, which mirrors the complexity and challenges found in real network environments, perform effectively well in real-world scenarios [42–46]. Because of incorporating over-the-air actual packets in a dedicated spectrum instead of simulated wire transmissions, datasets created using POWDER are analogous to real-world datasets. A detailed overview of POWDER is given in the appendix section C.

3 OVERVIEW

In this section, we discuss the scope, threat model, challenges, and requirements of FBSDetector.

3.1 Scope

The scope of FBSDetector is detecting FBSes and MSAs in the context of 4G cellular networks. There are two significant reasons for this. *First*, because of the extensive infrastructure already in place, 4G networks are widely accessible to a larger portion of the population. As of 2023, 4G adoption stands at 60% among 8.5 billion mobile connections [48–50]. 4G adoption is predicted to stay above 50% until 2027, and in 2029, 5G is expected to overtake 4G [51,52]. Therefore, until 2027, many end-user devices using 4G are at risk of FBS attacks. *Second*, the platform we use for real-world dataset generation for FBS and MSAs (i.e., POWDER) supports 4G functionalities and real-world experiments can be run in POWDER for different scenarios only in 4G. POWDER currently does not support all the 5G functionalities (for instance, handover). Our discussion with the POWDER team revealed that support for all 5G functionalities is in their plans. Nonetheless, extending FBSDetector to support 5G would require minimal effort once 5G support is available in POWDER because the high-level protocols of 4G and 5G are very similar. Therefore, the design of FBSDetector will remain the same.

3.2 Threat Model

This section outlines the key aspects of the threat model in the context of FBSes and MSAs.

FBS Deployment. The adversary can deploy FBSes in proximity to legitimate base stations. These FBSes may range from small to more sophisticated setups with varying transmission power.

Impersonation. FBSes can impersonate legitimate base stations by broadcasting signals that mimic the network identifiers (e.g., SSID) and encryption protocols used by legitimate base stations. However, the FBS does not know any cryptographic keys of the communication. By impersonating trusted networks, attackers can deceive mobile devices into connecting to FBSes.

MSA. Once UEs connect to the FBSes, adversaries can intercept and manipulate communication traffic. Adversaries may exploit vulnerabilities in the communication protocols by sending different out-of-sequence messages to perform different MSAs. Furthermore, they can change the MSA or re-shape attack traffic to evade detection.

Detection Evasion. Attackers may employ various techniques to evade detection. This includes rapidly changing the parameters of the FBSes, adjusting transmission power, or adopting sophisticated obfuscation methods to mask their activities.

3.3 Challenges

The challenges in designing our ML-based framework for detecting FBSes and MSAs are:

C1. Dataset Availability and Quality. Acquiring a comprehensive and high-quality dataset that encompasses a wide range of real-world cellular network scenarios is a significant challenge. The dataset must include instances of legitimate base stations, FBSes, and execution traces of different MSAs. Currently, there is no such dataset publicly available. There are several reasons behind this:

(1) The law prohibits the deployment of FBSes in public areas. If someone wants to deploy it for research and experimentation, they must do it in a controlled RF environment. (2) Incorporating different real-world cellular network scenarios, such as handovers and mobility, is a difficult task and would require a lot of specialized hardware and other equipment and facilities.

C2. Detecting FBSes from Packet Traces. Unlike traditional methods where packets themselves are inherently malicious, in the case of detecting FBSes, the true nature of a packet hinges on which context a packet was sent. For instance, the same packet with all the same contents can be sent by a base station or an FBS. Moreover, a critical constraint is maintaining the original sequence of packets as they were sent and received throughout the process to preserve the context information.

C3. Detecting MSAs. Recognizing MSAs from packet traces is even more challenging than FBS detection. These attacks have unique characteristics that define them. Moreover, MSAs often exhibit complex, evolving patterns that require careful observation to distinguish them from legitimate traffic. These attacks are notorious for their adaptability, constantly changing to evade detection. Consequently, our approach must evolve alongside these threats. We must capture these attack characteristics and represent them effectively in a structured data format.

C4. Combining NAS and RRC Predictions. Training our models separately on NAS and RRC layer packets is a necessary step due to their distinct features and characteristics. However, a challenge arises when we must consolidate these separate model predictions into a unified model. The challenge lies in harmonizing these diverse sets of predictions, ensuring that our final model can effectively capture the information of both layers while providing robust, accurate predictions.

C5. Real-Time Detection. Enabling real-time detection of FBSes and MSAs is a challenge due to the large volume and velocity of network traffic. The framework needs to be an in-device solution that captures, processes and analyzes incoming packet traces promptly to detect the presence of FBSes and MSAs effectively.

3.4 Proposed Solution

S1. We use different facilities available at POWDER [41] to create FBSAD and MSAD, real-world datasets to detect FBSes and MSAs. Designing different networking scenarios, we incorporate legitimate base stations and FBSes and collect data. We also collect network traces of different MSAs that use FBSes in their threat model. Different adversaries are incorporated for both FBSes and MSAs, from less sophisticated to more sophisticated, with the ability to clone legitimate base stations, change signatures, and turn on and off to evade detection. The dataset is then processed to make it appropriate for training different ML models. This includes protocol filtering, feature extraction, feature alignment, and replacing missing values.

S2. The lengths of the sequence of packets generated by FBSes follow a specific distribution (shown in Figure 7a and 7b). Based on this observation, we design a Sequential-LSTM model that takes sequence length as a hyperparameter and trains on chunks of packets. Another essential objective this design helps us achieve is incorporating the surrounding context into consideration. This approach

for FBS detection improves the detection accuracy and lowers the false positive rates more than any state-of-the-art model.

S3. We observe that each MSA shows a unique pattern if they are represented as a directed graph (see Figure 5 in Section 4.2.2). Based on this observation, we devise an innovative solution centered around graph data structures and learning techniques. We transform the packet traces into directed graphs. This graph representation captures the relationships inherent in the trace, which is ideal for detecting MSAs with complex and evolving patterns. We train a graph learning model specialized in learning complex patterns within the graph and learn the patterns of the MSAs. With the trained model, we can recognize the MSAs even if they evolve and unseen and reshaped attacks in our dataset with maximum overlapping sub-graphs.

S4. To combine the model predictions for RRC and NAS packets in FBS and MSA detection, we design a weighted confidence-based fusion method, a widely used technique in the multi-sensor information fusion field [53, 54]. The weights are assigned to the best model of each layer based on the model performance. This method offers a robust means to blend the predictions for NAS and RRC layer packets, facilitating the creation of a unified and accurate predictive framework that captures the strengths of each layer.

S5. The development of a mobile app emerges as a pragmatic solution for deploying the FBSDetector for real-time detection. Such a dedicated app would serve as an in-device solution, capable of swiftly capturing, processing, and analyzing incoming packet traces with on-device ML models, specifically tailored for detecting FBSes and MSAs. Regular model updates would ensure adaptability to threats and new and unseen attacks.

4 DETAILED DESIGN

In this section, we discuss the detailed design of FBSDetector (see Figure 3 for an overview). On a high-level, the design of FBSDetector is divided into three components: (1) Dataset Construction, (2) ML Framework, and (3) Deployment.

4.1 Dataset Construction

Our dataset construction process is described below.

4.1.1 Dataset Generation. We create cellular networks in POWDER incorporating legitimate base stations, FBSes, and MSAs, run experiments, and capture the packets from all the cellular network components to generate the dataset.

Mobility. One real-world phenomenon in cellular networks is the mobility of the UEs. Signal strengths of base stations received at UEs moving from one place to another vary, causing the UEs to be handed over from one base station to another. Incorporating this scenario in the dataset is important; otherwise, a benign handover due to mobility might be interpreted as malicious. With the help of mobile endpoints available at POWDER, we incorporate this scenario into our dataset.

Attacker Ability. The attackers we consider have a diverse set of abilities, from less sophisticated to more sophisticated. Based on their abilities, we can rank them in five levels, level 0 being the least sophisticated and level 4 being the most sophisticated.

- **Level 0:** Attackers only set up FBSes naively with a high signal strength.

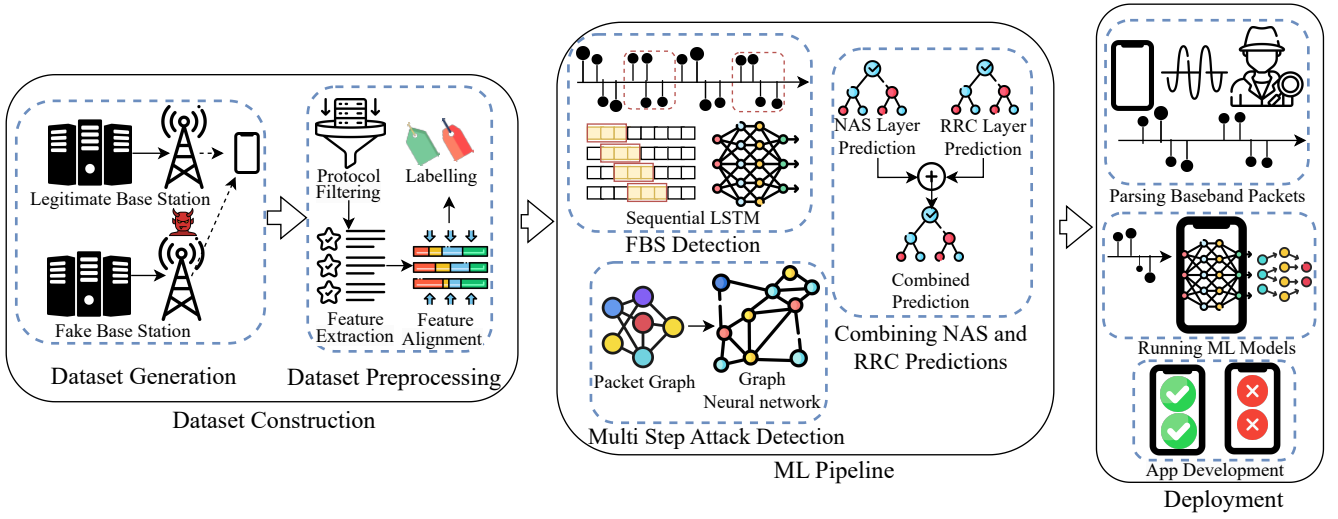


Figure 3: Overview of FBS-Detector

| Layer | Attack | Ref |
|-------|----------------------------------|------|
| RRC | Energy Depletion Attack | [7] |
| | Paging Channel Hijacking Attack | [7] |
| | Panic Attack | [7] |
| | Stealthy kicking-off Attack | [7] |
| | Incarceration Attack | [9] |
| NAS | Numb Attack | [7] |
| | Detach/Downgrade Attack | [7] |
| | Uplink NAS Counter Desync Attack | [9] |
| | Downgrade Attacks | [55] |

Table 1: Multi-Step Attacks using FBS

- **Level 1:** Attackers set up FBSes with an optimal signal strength sufficient to trigger a handover in the UEs.
- **Level 2:** Attackers can clone all the parameters of a legitimate base station and impersonate the legitimate base station.
- **Level 3:** Attackers can carry out usual MSAs.
- **Level 4:** Attackers can change the typical attack signatures that the FBSes and MSAs follow and reshape traffic. Attacks can be reshaped by changing the packet orders and packet fields. It is known that there are typical defenses deployed and the attackers actively aim to evade them.

MSA Data Generation. To create MSAD, we chose several attacks that are executed in multiple steps and use FBS in their threat model. As shown in Table 1, we have selected 9 attacks, which are representative of the most popular MSAs. These attacks cover a wide range of practical threats, including DoS, privacy leakage, and downgrade, which can be quickly launched to compromise practical networks and devices severely. We implement and execute these attacks in the cellular networks in POWDER and incorporate instances of each attack in MSAD.

4.1.2 Dataset Preprocessing. In order to make FBSAD and MSAD suitable for training ML models, we pre-process them in several steps.

Protocol filtering, field extraction and alignment. Each packet in the network trace contains multiple protocol information. We focus on only NAS and RRC data and use protocol filtering to isolate the relevant packets precisely. We further extract the values of fields associated with these packets. A challenge is the presence of varying field counts among different packets; to address this, we align the packets based on their shared field values. This process ensures consistency in our dataset, enabling uniformity in subsequent analyses and modeling.

Handling missing values. The alignment of packets based on shared field values, when specific fields are disjoint across packets, results in missing values within the dataset– a scenario that cannot be resolved using conventional methods like mean or median imputation, as packet features lack a typical distribution. To tackle this issue and ensure data completeness, we replace the missing values with a flag value of -1 to indicate their absence. This uniform marker across the dataset is a pragmatic solution, allowing us to retain valuable features without introducing bias or compromising data quality.

Encoding the categorical values. In our dataset, numerous fields take on categorical values, which hinders the model’s understanding. We thus encode the categorical fields to numerical representations to make them suitable for training ML models.

4.1.3 Dataset Labelling. The datasets are labeled according to their reason for generation. Formally, for a packet \mathcal{P} we define the following formulation:

Let,

$$\text{FBSAD} := \langle X_{\text{FBSAD}}, Y_{\text{FBSAD}} \rangle$$

where X_{FBSAD} are the packet features, Y_{FBSAD} are the packet labels and,

$$i \in \{1, n_{\text{FBSAD}}\}, \text{ where } n_{\text{FBSAD}} = |X_{\text{FBSAD}}|$$

$$\vec{x}_{\text{FBSAD}}^{(i)} \in X_{\text{FBSAD}}, \vec{y}_{\text{FBSAD}}^{(i)} \in Y_{\text{FBSAD}}$$

then we can label each packet $\vec{x}_{\text{FBSAD}}^{(i)}$ as

$$\vec{y}_{\text{FBSAD}}^{(i)} = \begin{cases} 0 & \text{if } \vec{x}_{\text{FBSAD}}^{(i)} \text{ is a benign packet} \\ 1 & \text{if } \vec{x}_{\text{FBSAD}}^{(i)} \text{ is generated from FBS} \end{cases}$$

For MSAD, we define $\mathcal{A} := \{\text{attack}_1, \text{attack}_2, \dots, \text{attack}_k\}$ as the set of MSAs detected by FBSDetector where k is the number of MSAs that can be detected and $\mathcal{L}_{\mathcal{A}} := \{0, 1, 2, \dots, k\}$ as the set of labels for the MSAs. Let,

$$\text{MSAD} := \langle X_{\text{MSAD}}, Y_{\text{MSAD}} \rangle$$

where X_{MSAD} are the packet features, Y_{MSAD} are the packet labels and

$$i \in \{1, n_{\text{MSAD}}\}, \text{ where } n_{\text{MSAD}} = |X_{\text{MSAD}}| \\ \vec{x}_{\text{MSAD}}^{(i)} \in X_{\text{MSAD}}, \vec{y}_{\text{MSAD}}^{(i)} \in Y_{\text{MSAD}}$$

then we can label each packet $\vec{x}_{\text{MSAD}}^{(i)}$ as

$$\vec{y}_{\text{MSAD}}^{(i)} = \begin{cases} 0 & \text{if } \vec{x}_{\text{MSAD}}^{(i)} \text{ is a benign packet} \\ \mathcal{L}_{\mathcal{A}}[\text{attack}_j] & \text{if } \vec{x}_{\text{MSAD}}^{(i)} \text{ is generated} \\ & \text{by } \text{attack}_j \in \mathcal{A} \end{cases}$$

4.2 Machine Learning Framework

In what follows, we detail the ML framework used in FBSDetector.

4.2.1 FBS Detection. FBSes generate a sequence of messages, and detecting a single packet often leads to classification errors due to lack of context. Following these observations, we design a Sequential-LSTM model that takes the length of the sequence into account (shown in Algorithm 1). The algorithm essentially divides the dataset into chunks of sequences using sequence length (len_{seq}) as a hyperparameter and returns a Seq-LSTM model trained on these sequences. This approach can help us learn better from the context of a chunk with the information about an FBS communication, improve the detection accuracy, and reduce the false positive rate.

4.2.2 MSA Recognition. MSAs can be uniquely represented as directed graphs and detected using graph learning. We describe the steps to create a directed graph from the traffic dataset and graph learning in Algorithm 1. The algorithm constructs a directed graph from the packets - each node denoting a packet, each packet having a directed edge towards the next packet. Edges are labeled with their reason for generation, the same as the packet label, generated as part of a benign flow or in the path of an MSA. Lastly, a graph learning model learns and generalizes this knowledge from the graphs, and the model is finally returned. Recognizing MSAs using graph learning approaches can be formally represented as follows. Let $G = (V, E)$ represent the graph constructed from the packets, where each node V denotes a packet. E represents the directed edges between nodes in the flow graph. An MSA is recognized by identifying a specific path $P(G)$ corresponding to \mathcal{A} within the graph G . These paths represent the packets' sequences that follow an MSA pattern. If there is an evolving and unseen attack, the attack would deviate from path $P(G)$ and follow a different path $P'(G)$. Due to the nature of the vulnerabilities exploited by the attackers, $P'(G)$ and $P(G)$ will not be completely edge-disjoint and will have

Algorithm 1 FBS and MSA Learning Algorithms

```

1: Input: Hyperparameter:  $len_{seq}$ .
2: Labeled dataset: FBSAD, MSAD
3: Output: Seq-LSTM model, Graph Model (GM)
4: procedure FBS TRAINING
5:   Divide FBSAD into  $\frac{|FBSAD|}{len_{seq}}$  chunks  $C$ 
6:   for  $c$  in  $C$  do
7:     Train the Seq-LSTM model on  $c$ 
8:   end for
9: end procedure
10: procedure GRAPH LEARNING
11:   Variables: Graph  $G(V, E)$ 
12:   Create start node  $V_1$  with the first packet  $p_1$ 
13:   for each subsequent packet  $p_i$  in MSAD do
14:     if  $V_p$  not in  $G$  then
15:       Create a node  $V_p$ 
16:     end if
17:     Add an incoming edge  $E_p$  from  $V_{p-1}$  to  $V_p$ 
18:     Label  $E_p$  with  $L_p$ , the Label for Packet  $p$ 
19:   end for
20:    $GM = \text{train}(G)$ 
21: end procedure
22: return Seq-LSTM, GM

```

overlaps. From these overlaps, we can detect evolving, unseen and reshaped attacks.

MSA Detection Example. To further illustrate the process of MSA detection, we discuss the paging channel hijacking attack, its attack flow, and how it is converted to a graph to be utilized by graph learning algorithms.

Paging Channel Hijacking: To hijack the paging channel of the victim UE and the legitimate base station, the FBS broadcasts fake empty *paging message* in the shared paging channel with higher signal power. Upon receiving the *Paging request*, the victim UE detaches itself from the legitimate base station and connects to the FBS. This attack diagram is shown in Figure 4 and Figure 5 shows the graph generated from this attack. The communication starts when a UE sends a *AttachRequest* message to the legitimate base station, which is the starting node of the graph. An incoming edge is added to the node that represents the message for the subsequent messages. The graph enters into an attack sequence when a *paging(empty)* message is sent after the *AttachComplete* message. Communication terminates when a *DetachRequest* message is sent; this is the terminating node of the graph.

4.2.3 Combining NAS and RRC Predictions. To combine the predictions from the NAS and RRC layer models, we leverage the Dempster-Shafer theory (DST) [56] to facilitate the fusion of predictions. We employ a weighted confidence-based fusion method, where weights are assigned to the best model of each layer based on the model performance. Let W_{NAS} and W_{RRC} represent the weights assigned to the best models of NAS and RRC layer, $P = \{P_{NAS}, P_{RRC}\}$ represent the predictions made by those models, and P_W is the final prediction. We assign weights W_{NAS} and W_{RRC} proportional to their support scores on the inference. The more confident model among the two models receives a higher weight, indicating a more

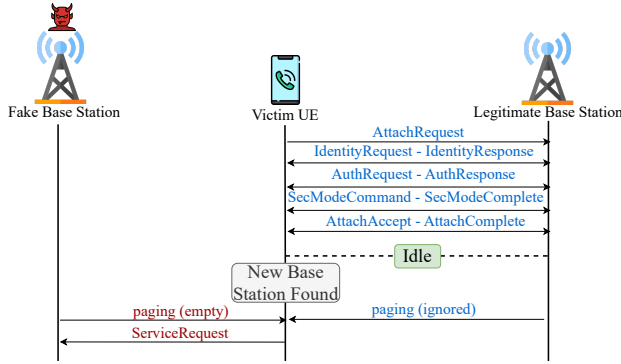


Figure 4: Paging Channel Hijacking Attack Diagram

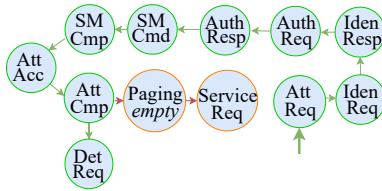


Figure 5: Graph of paging channel hijacking attack

significant influence on the combined prediction. Mathematically, this is expressed as:

$$W_{NAS} \propto \text{Support_Score}(P_{NAS}) \text{ and } W_{RRC} \propto \text{Support_Score}(P_{RRC})$$

When there's a disagreement between the models, the Dempster-Shafer theory is applied, and the prediction with higher confidence gets priority. This process is formalized as:

$$P_W = \begin{cases} P_{NAS} & \text{if } P_{NAS} = P_{RRC} \\ P_{NAS} & \text{if } P_{NAS} \neq P_{RRC} \text{ and } W_{NAS} > W_{RRC} \\ P_{RRC} & \text{if } P_{NAS} \neq P_{RRC} \text{ and } W_{NAS} < W_{RRC} \end{cases}$$

Combining the predictions in this way yields a better detection accuracy than the individual predictions.

5 IMPLEMENTATION

Now, we discuss the implementation details of each component of FBSDetector. We formulate two distinct models: one designed to detect FBSes and another specifically tailored to recognize MSAs. Implementation efforts of FBSDetector are summarized in Table 2.

5.1 Dataset Construction

Incorporation of Fake Base Stations. To incorporate FBSes, we create (i) a legitimate core network and base station pair and (ii) a fake core network and base station pair in POWDER. The legitimate base station serves UEs that the FBS can attack by spawning near it with higher signal strength. The core networks use Open5GS [57] to support handover, and both the base stations and the UE use srsRAN [58]. Following our threat model, the FBS core network

| Task | Framework | Lang | Libraries Used | LoC |
|------------------------------|-----------|--------|------------------------------------|-----|
| Handover capability in srsUE | srsRAN | C | | 316 |
| MSAs | srsRAN | C | | 542 |
| Data Processing | | Python | tshark, scikit-learn | 72 |
| Training ML Models | | Python | scikit-learn, TensorFlow | 40 |
| Sequential LSTM | | Python | scikit-learn | 42 |
| Graph Learning Pipeline | | Python | networkx, pytorch-geometric | 70 |
| App Development | Flutter | Dart | mobileinsight-lib, tensorflow-lite | 290 |

Table 2: Implementation efforts

does not know the cryptographic keys. To incorporate less sophisticated attackers, we only set up an FBS with a fixed high signal strength value in the configuration. In contrast, to incorporate more sophisticated attackers, we clone legitimate base station IDs and different parameters, change signatures and signal strength, and turn them on and off to evade detection. We introduce mobility in the dataset by using UEs with the mobile endpoints in POWDER that are mounted in the campus shuttles. Benign handovers are initiated when a shuttle with a mobile endpoint moves from the vicinity of one base station to another, and the signal quality received at the UE changes. To initiate a fake handover through FBSes, we spawn an FBS near a UE with high signal strength and make the UE initiate an unsuccessful handover. We combine all these scenarios in our experiments, listed in Table 9.

Implementation of handover capability in the srsUE. The UEs usually initiate handovers by sending a *TrackingAreaUpdateRequest* message. This message is not implemented in the current release of srsRAN. We implement the *TrackingAreaUpdateRequest* message in srsUE and make it able to initiate a handover request by sending a *TrackingAreaUpdateRequest* message.

Implementation and Execution of MSAs. We implement all the attacks listed in Table 1 in srsRAN and execute them in the experimental setup we created in POWDER. For a less sophisticated attacker, we implement the MSAs in srsRAN as their definition, but for a more sophisticated attacker, we reshape the packets in srsRAN and change the attack patterns by changing the packet sending orders. All the traces from different components are captured for both NAS and RRC layer.

Data Processing: We decode the packets using tshark [59]. and use a Python script for protocol filtering, packet field extraction, packet alignment, and handling missing values. Lastly, we use *scikit-learn's LabelEncoder* to encode the categorical fields into numerical representations.

Data Labeling: We store the predefined attack labels in a dictionary and assign each packet a label according to their reason for generation. The NAS layer packets (fewer in number) are labeled with a script that checks each packet and assigns a label according to the dictionary. The RRC layer packets (which are much more numerous) are labeled in batches of intervals by detecting attack intervals in the NAS layer packet sequences. There are only two labels (benign and malicious) for the FBS dataset, whereas the MSA dataset has multiple labels, one for each type of attack and one for benign packets. Like before, we design a script that labels the malicious packets with a different MSA-specific label for the attack it was generated from.

5.2 FBS Detection

Train-Test Split. We use a Python script to split our experimental dataset for training and testing that does roughly 80 – 20 split preserving the sequence of packets. For example, if we have 10 instances of the FBS experiment, we append 8 experiment’s data to the train set and 2 to the test set. This way we preserve the sequence of packets while ensuring the standard split, also no experimental trace is cut in between.

Training Models. For training the *Sequential-LSTM*, we use a custom training pipeline in Python that takes sequence length as a hyperparameter. All the libraries used to train the ML models are listed in Table 2.

5.3 MSA Recognition

For NAS layer packets, we create a node for every unique value of the `nas_eps_nas_msg_emm_type_value` field, the packet name for NAS layer packets. Similarly, for the RRC layer packets, we create a node for every unique value of the `lte-rrc_c1_showname` field, which is the packet name for the RRC layer packets. Every packet maps to a node in the graph corresponding to its packet name. We add an edge from the node representing one packet to the node representing the next packet in the sequence and label that edge with the same label we labeled the next packet. This denotes if the transition was benign or due to an attack. The containers and libraries to create the directed graphs and graph learning are summarized in Table 2.

5.4 Deployment and Integration

To deploy FBSDetector, we use Mobileinsight [60] to parse the baseband traces in the mobile phones, *TensorflowLite* [61] to run the ML models, and *Flutter* [62] to build the app.

6 EVALUATION

We evaluate the effectiveness of FBSDetector based on the following research questions:

- RQ1.** What is the distribution of the dataset, and what key features can be extracted from the dataset?
- RQ2.** Why a sequential model is essential for FBS detection? How does the weighted confidence-based fusion method for combining predictions of NAS and RRC packets further improve performance? How does graph learning improve MSA recognition performance?
- RQ3.** What is the memory and power consumption of the detection pipeline? How much time does the inference take?
- RQ4.** Was FBSDetector deployed and tested in a real-world setup? How does it contrast with existing FBS detection solutions?
- RQ5.** Is FBSDetector robust and generalizable against reshaping and unseen attacks?

In what follows, we delve into the details and answers to those research questions.

6.1 RQ1. Characteristics, Distribution, Feature, and Patterns of the Dataset

To identify the characteristics and gain insights about the dataset, we show different distributions of the packets in our dataset.

Total number of packets. There are 1662 NAS layer packets in the FBS dataset in total, 907 benign and 755 malicious, and there are 339813 RRC layer packets in total, 338195 benign and 1618 malicious. For the MSA dataset, there are 16804 NAS layer packets, 502 benign and 15962 malicious, and there are 393684 RRC layer packets, 338195 benign and 1618 malicious. The detailed distributions are shown in Table 10 and 15 in appendix section A. From the distributions, we can see that the number of packets during different experiments is consistent, that is, the number of benign and malicious packets is in a certain proportion in both NAS and RRC layers and they do not deviate much from this proportion. This shows the consistency in our dataset.

Distribution of different NAS and RRC layer packets. We can see the distribution of NAS and RRC layer packets in the combined FBS detection dataset in Table 11 and 12 respectively in the Appendix Section A. Figure 6a and 6b show this distribution graphically. The same observation can be made from the distribution of MSA packets in Table 13 and 14 and Figure 6c and 6d.

FBS sequence length. The distribution of FBS sequence length in the NAS and RRC layer is shown in Figure 7a and 7b. The figures show that for NAS layer packets, most sequences are between 8 and 20. For RRC layer packets, it is between 80 and 120. This is a significant observation because sequence length is a hyperparameter of our model, and its performance depends mainly on tuning this hyperparameter properly. We discuss the impact of sequence length on model performance in our answer to RQ2.

6.2 RQ2. Sequential Training, Graph Learning, Predictions Combining

Sequential Training for a More Accurate Detection of FS-Bes. Like legitimate base stations, FBSes generate sequences of messages. Figures 7a and 7b show the distribution of the length of the sequences. As mentioned in Section 4, to take into account the context for each packet, we use a Sequential-LSTM model taking the sequence length as a hyperparameter. The experimental results reported in Table 3 demonstrate the superior performance of this approach over other models. Though Sequential-LSTM outperforms its closest competitor XGBoost, in detecting NAS layer packets with a small improvement in F1-Score and accuracy (2%), the most substantial enhancement is observed with a 6% increase in recall. Improving recall in malicious traffic classification means the model is better at capturing a larger proportion of actual threats, reducing the chances of missing malicious activity. This is crucial for minimizing false negatives and enhancing overall detection effectiveness. Figures 7c and 7d show the impact of sequence length on the detection performance. Models perform better when the sequence length is between 9 – 15 for NAS layer packets and 80 – 120 for RRC layer packets. This is because, in an FBS session, based on the communication process of the FBSes, packets exchanged between the FBSes and the UEs in the NAS and RRC layer follow a specific pattern. These patterns are captured better when the sequence lengths are set in the range that can accommodate the patterns completely, and models trained on these chunks of packets that contain these patterns can sufficiently learn better about the attack.

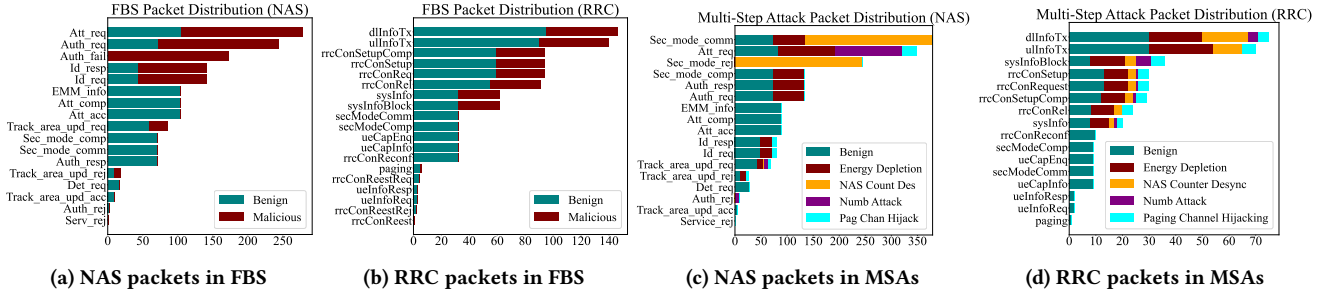


Figure 6: Distribution of NAS and RRC packets in FBSAD and MSAD

| Model | NAS | | | | RRC | | | |
|------------------------|-------------|-------------|-------------|-------------|-------------|-------------|-------------|-------------|
| | Precision | Recall | F1-Score | Accuracy | Precision | Recall | F1-Score | Accuracy |
| Random Forest | 0.85 | 0.97 | 0.82 | 0.84 | 0.68 | 0.81 | 0.16 | 0.69 |
| SVM | 0.81 | 0.21 | 0.70 | 0.59 | 0.66 | 0.79 | 0.00 | 0.66 |
| Decision Tree | 0.86 | 0.90 | 0.81 | 0.82 | 0.75 | 0.84 | 0.53 | 0.76 |
| XGBoost | 0.89 | 0.91 | 0.84 | 0.84 | 0.93 | 0.87 | 0.79 | 0.84 |
| k-NN | 0.86 | 0.81 | 0.80 | 0.79 | 0.86 | 0.89 | 0.82 | 0.87 |
| Naive Bayes | 0.53 | 0.97 | 0.35 | 0.58 | 0.90 | 0.08 | 0.52 | 0.37 |
| Logistic Regression | 0.50 | 0.68 | 0.69 | 0.53 | 0.74 | 0.85 | 0.50 | 0.71 |
| CNN | 0.86 | 0.39 | 0.57 | 0.52 | 0.94 | 0.67 | 0.78 | 0.66 |
| FNN | 0.79 | 0.85 | 0.68 | 0.73 | 0.80 | 0.88 | 0.84 | 0.78 |
| LSTM | 0.86 | 0.65 | 0.72 | 0.71 | 0.89 | 0.56 | 0.71 | 0.59 |
| Sequential-LSTM | 0.89 | 0.97 | 0.86 | 0.86 | 0.94 | 0.97 | 0.95 | 0.91 |

Table 3: Performance of ML models in FBS detection from NAS and RRC layer packets

| Model | Precision | Recall | F1-Score | Accuracy |
|----------------------------|-------------|-------------|-------------|-------------|
| Sequential-LSTM (NAS) | 0.89 | 0.97 | 0.86 | 0.86 |
| Sequential-LSTM (RRC) | 0.94 | 0.97 | 0.95 | 0.91 |
| Combined Prediction | 0.96 | 0.98 | 0.97 | 0.92 |

Table 4: Performance of FBS detection after combining predictions

Graph Learning in MSA Recognition. MSAs follow specific patterns, as shown in Figure 5. We train graph learning models to learn these patterns, and Table 5 shows that learning the patterns, the graph learning models perform better than any other models in recognizing MSAs, GraphSAGE performs the best among all. So we use GraphSAGE as our MSA recognition model. Though the improvement seen in accuracy might seem small (1%), a significant improvement is seen in precision (4-8%), recall (10-12%) and f1-score (8-10%). It is worth noting that Sequential-LSTM also achieves competitive performance compared to the other ML models.

Weighted Confidence-based Fusion Method for Combining Predictions. The performance after combining the predictions of NAS and RRC packets using the weighted confidence-based fusion method for FBS detection and MSA recognition are shown in Table 4 and Table 6, respectively. Leveraging knowledge from both layers, this method improves all the performance metrics from the best model among the two and makes the system robust, especially by improving recall.

Experimental Setup. We provide detailed information about the experimental setup, including the training hardware specifications and model hyperparameters, in Appendix Section B.

| Model | NAS | | | | RRC | | | |
|-----------------------------|--------------|--------------|--------------|-------------|--------------|--------------|--------------|-------------|
| | Precision | Recall | F1-Score | Accuracy | Precision | Recall | F1-Score | Accuracy |
| Random Forest | 0.617 | 0.628 | 0.454 | 0.76 | 0.343 | 0.278 | 0.254 | 0.42 |
| SVM | 0.088 | 0.200 | 0.122 | 0.44 | 0.076 | 0.200 | 0.110 | 0.38 |
| Decision Tree | 0.342 | 0.402 | 0.356 | 0.66 | 0.076 | 0.200 | 0.110 | 0.38 |
| XGBoost | 0.794 | 0.573 | 0.786 | 0.84 | 0.586 | 0.530 | 0.548 | 0.47 |
| k-NN | 0.734 | 0.702 | 0.706 | 0.81 | 0.484 | 0.454 | 0.392 | 0.47 |
| Naive Bayes | 0.440 | 0.384 | 0.274 | 0.29 | 0.440 | 0.258 | 0.178 | 0.11 |
| Logistic Regression | 0.088 | 0.200 | 0.122 | 0.44 | 0.412 | 0.318 | 0.300 | 0.49 |
| CNN | 0.132 | 0.274 | 0.114 | 0.22 | 0.072 | 0.259 | 0.106 | 0.36 |
| FNN | 0.128 | 0.282 | 0.222 | 0.24 | 0.274 | 0.220 | 0.144 | 0.40 |
| LSTM | 0.150 | 0.320 | 0.200 | 0.49 | 0.128 | 0.164 | 0.130 | 0.30 |
| Sequential-LSTM | 0.744 | 0.726 | 0.784 | 0.85 | 0.408 | 0.342 | 0.348 | 0.53 |
| Graph Attention Network | 0.868 | 0.672 | 0.865 | 0.84 | 0.316 | 0.338 | 0.298 | 0.36 |
| Graph Attention Network v2 | 0.842 | 0.864 | 0.857 | 0.83 | 0.504 | 0.411 | 0.421 | 0.42 |
| Graph Convolutional Network | 0.832 | 0.754 | 0.818 | 0.80 | 0.306 | 0.464 | 0.352 | 0.40 |
| Graph Transformer | 0.836 | 0.882 | 0.841 | 0.81 | 0.436 | 0.495 | 0.430 | 0.41 |
| GraphSAGE | 0.872 | 0.924 | 0.883 | 0.85 | 0.633 | 0.561 | 0.557 | 0.59 |

Table 5: Performance of MSA recognition from NAS and RRC layer packets

| Model | Precision | Recall | F1-Score | Accuracy |
|----------------------------|--------------|--------------|--------------|--------------|
| GraphSAGE (NAS) | 0.867 | 0.879 | 0.856 | 0.850 |
| GraphSAGE (RRC) | 0.611 | 0.480 | 0.52 | 0.590 |
| Combined Prediction | 0.875 | 0.901 | 0.874 | 0.865 |

Table 6: Performance of MSA recognition after combining predictions

6.3 RQ3. Overhead Analysis: Time Consumption, Memory Consumption, Power Consumption

We evaluate the overhead of FBSDetector based on several criteria. Figure 8a shows the time required to predict packets, which increases linearly with the number of packets. The slope of the increase is minimal, which means that the solution can scale to high throughput applications. Figure 8c shows the memory consumption and Figure 8b shows the power consumption of FBSDetector, consumed in packet processing and running ML model on the processed packets to generate inference. The trend of power consumption is also linearly increasing, with a small slope and the trend of memory consumption is decreasing, which can result from multiple hardware-level optimizations by the operating system. Compared to a recent approach [3], which uses an average of 4 mW power, FBSDetector uses less than 2 mW of power to detect an FBS. These results show that FBSDetector is a promising solution for deployment in real-world systems, having negligible overhead.

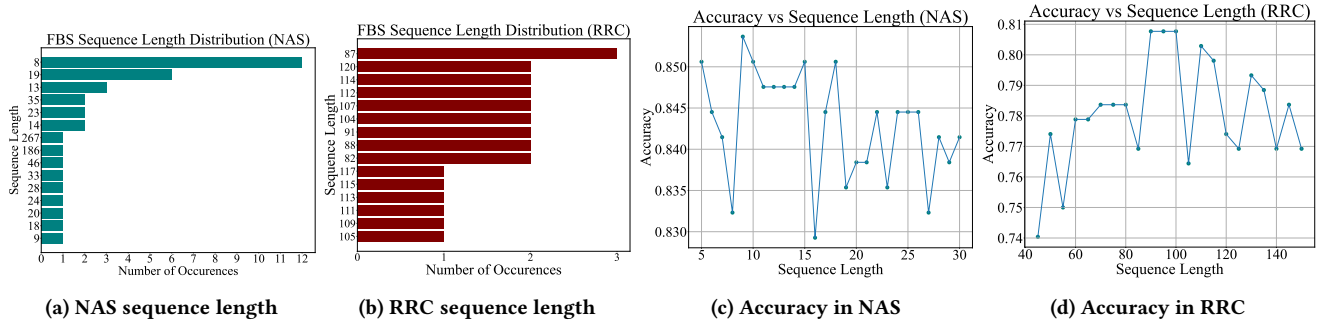


Figure 7: Distribution and impact of NAS and RRC sequence length in FBS detection

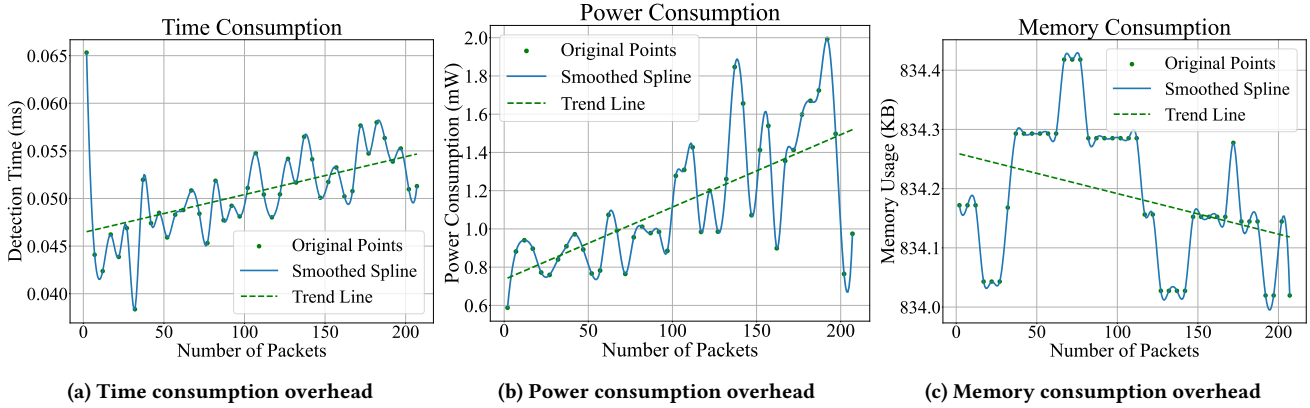


Figure 8: Performance overhead of FBSDetector

6.4 RQ4. Real-World Validation and Comparison with Existing Solutions

Real-world validation. To validate FBSDetector’s performance against threats in the wild in real environments, we create a testbed in our controlled lab environment. We used (1) One USRP B210 [63], (2) One engineering laptop and (3) a Google Nexus 5 smartphone with a Google Fi sim card that has the FBSDetector app installed. We used Open5GS [57] for the core network and srsRAN [58] for the base station. Following the standard approaches, we create and spawn an FBS using the laptop as the core network and the USRP B210 SDR as the base station. We place the FBS near the smartphone with the FBSDetector app, run experiments with different scenarios for FBS detection and MSA recognition and measure detection performance. We test with (1) varying attacker capabilities (from less sophisticated to more sophisticated), (2) mobility (limited within the lab environment), (3) benign handovers and FBS handover attempts, (4) unseen attacks, and (5) reshaped attacks. The results are analogous to the similar experiments we conducted in POWDER.

Comparison with existing solutions. We compare FBSDetector with different real-world solutions. The criteria for the comparison are: (1) The solution must not require any changes in the protocol. (2) The source of the solution must be available and maintained. (3) No additional hardware is required for operation. The comparison

| Solution | Supports 4G | No Change in Protocol | No Additional Hardware Required | Source Available | Detects FBS |
|---------------------------|-------------|-----------------------|---------------------------------|------------------|-------------|
| Crocodile Hunter [23] | ✓ | ✓ | ✗ | ✗ | - |
| Darshak [30] | ✗ | - | - | - | - |
| Baron [32] | ✓ | ✗ | - | - | - |
| Phoenix [3] | ✓ | ✓ | ✓ | ✗ | - |
| Android IMSI Catcher [31] | ✓ | ✓ | ✓ | ✓ | ✗ |
| SnoopSnitch [33] | ✓ | ✓ | ✓ | ✓ | ✗ |
| FBSDetector | ✓ | ✓ | ✓ | ✓ | ✓ |

Table 7: Comparison of FBSDetector with existing solutions summary in Table 7 shows that only Android IMSI Catcher (AIMSICD) [31] and SnoopSnitch [33] satisfy all comparison criteria. So we test them in our testbed by creating an FBS in our controlled lab environment and spawning it near a mobile device with AIMSICD and SnoopSnitch installed and running. We ran the experiment several times, but neither of the solutions could detect the FBS, whereas FBSDetector detected the FBS every time.

6.5 RQ5. Detecting Unseen and Reshaped Attacks: Robustness and Generalizability

To establish a benchmark and prove the robustness and generalizability of FBSDetector, we evaluate its capability to detect unseen and reshaped attacks.

Unseen Attacks: FBSDetector can detect unseen attacks by leveraging anomalies in behavior that deviate from benign patterns. In cases where it encounters an attack it has not seen before, there will be a misclassification into an existing class. However, the attack

| Classified as | Unseen Attack Detection | | | Reshaped Attack Detection | | |
|--------------------------|-------------------------|------------------|-------|---------------------------|-----------------------------------|-------|
| | Benign | Stealthy Kickoff | Total | Benign | Reshaped Paging Channel Hijacking | Total |
| True labels | 133 | 65 | 198 | 145 | 95 | 240 |
| Benign | 128 | 3 | 131 | 136 | 5 | 141 |
| Paging Channel Hijacking | 3 | 56 | 59 | 6 | 82 | 88 |
| Numb Attack | 2 | 6 | 8 | 2 | 6 | 8 |
| Panic Attack | | | | 1 | 2 | 3 |

Table 8: Unseen and reshaped attack detection

would not go undetected, as the deviation from established benign behavior will still trigger an alert, ensuring that all anomalies are identified and addressed. We test this by keeping the stealthy kickoff attack data unseen during training. Table 8 shows that most of the unseen attack packets (86.15%) are classified as paging channel hijacking attacks, closest to the stealthy kickoff attack. This proves the capability of FBSDetector to detect unseen attacks and to generalize.

Reshaped Attacks: In case of attack reshaping, especially for attackers with more sophisticated capabilities, even if the attacker is aware of the presence of FBSDetector and reshapes the MSA completely to evade detection, FBSDetector can still detect it. This reshaped behavior deviates from benign behavior and overlaps with the original attack that was reshaped, and FBSDetector is able to detect it from this deviation and overlap. To test FBSDetector’s capability to detect reshaped attacks properly, we reshape the paging channel hijacking attack by changing different fields in the paging messages and changing the paging intervals. Table 8 shows that most of the reshaped attack packets (86.32%) are classified as paging channel hijacking attacks, which is the original attack. This proves the capability of FBSDetector to detect reshaped attacks.

7 RELATED WORK

Several approaches have been proposed to address the challenge of detecting FBSes. We now present an overview of those approaches and highlight their key contributions and limitations.

Fake base station detection and defense. The approaches proposed in [34, 35] require installing expensive hardware and in most cases they are proprietary. The techniques in [3, 23, 30, 31, 33] are based on several simple heuristics and signatures which often entail high false positive rates. The approach in [29] depends on crowd-sourced data, which is not a practical solution for scaling up. ML based efforts are effective in detecting attacks and anomalies from traces [19, 27, 28]. However, they work on small datasets generated in simulated environments that lack diversity; also because they work only in the data plane, they cannot detect MSAs. Previous works have shown that information related to the connection between a UE and a base station can be used to reason about the authenticity of the base station [20–22, 24–26, 29, 64]. However, these solutions require changes to the protocol and additional hardware. Recent efforts have introduced certificate-based solutions and digital signatures [15–17, 19] for base station authentication. In [4, 16, 32], the authors propose a defense methodology to enable UEs to determine whether a base station is legitimate or fake by efficient broadcast authentication protocol. These techniques introduce additional authentication methods requiring critical specifications modifications and add overhead.

Cellular network security. Over the years, several research efforts have focused on the security of cellular networks. DoLTest [5]

introduced an in-depth downlink negative testing framework for 4G devices. LTEFuzz [6] extensively investigates the security aspects of control plane procedures in 4G networks. Methods for stealthy tracking and eavesdropping are introduced in [47, 65]. Authors in [11, 66] demonstrate adaptive physical overshadowing attacks in cellular networks. REVOLTE [67] exploits an LTE implementation flaw to recover the contents of an encrypted VoLTE call and discuss short and long-term countermeasures. A comprehensive layer two security analysis is conducted by [68] and a proof-of-concept 5G SUCI-Catcher attack is demonstrated by [14]. The unmitigated handover vulnerabilities and potential countermeasures are studied by [69]. Klischies et al. [70] systematically discover undefined behavior in cellular specifications. IMP4GT [71] analyzes missing integrity protection of the user plane in mutual authentication protocol. Through different types of documentation analysis, Chen et al. [72–74] discover vulnerabilities in cellular network protocols automatically. The authors in [8, 75–77] study the simultaneous practical attacks against privacy and availability in multiple cellular networks. The capability to abuse 5g’s warning and emergency systems is demonstrated by [78]. Karakoc et al. analyze bidding-down attacks [55]. Frameworks for protocol analysis [7, 9, 79] and implementation analysis [80] aim to find inconsistencies in specifications and implementations that can lead to critical vulnerabilities. The exploitation and protection of the paging protocol are investigated in [10, 15]. Despite these efforts, detecting FBSes remains a challenging problem due to the ineffectiveness and impracticality of the existing solutions against the rapid evolution of attack techniques.

8 DISCUSSION

Applicability to 5G. To the best of our knowledge, no open-source protocol stack for the standalone 5G core network supports handover, which is a prerequisite for experimenting with FBSes and conducting FBS-based MSAs. Therefore, we leave the detection of FBSes and MSAs in 5G cellular networks with FBSDetector as a future work. However we believe that, based on 4G, our approach is equally applicable to 5G. For example, like 4G, 5G has a multi-layer design with most of the procedures unchanged from 4G. Thus, the multi-layer protocol filtering, distribution and sequence of packets, and other insights will largely remain the same when porting FBSDetector to 5G.

Ethical Considerations. Safe practices were always employed during the experiments in the controlled lab environment. The experiments involving radio frequencies were conducted inside a Faraday cage. Only authorized personnel with the testing devices were allowed inside the lab. The authors used their SIM cards for the experiments, and they did not face any problems using the SIM cards afterward. To maintain ethical standards in the FBSDetector app while capturing packets, it asks for consent from its user before each operation. User data confidentiality is a top priority, with robust encryption and storage measures in place. An opt-out option ensures user autonomy. The app is committed to aligning with ethical principles, prioritizing user trust and privacy.

Recent efforts by companies to defend FBS. In 2021, Google released an optional feature for Android to turn off the ability to connect to 2G cell sites [38]. Google announced another new mobile security setting for Android which allows users to prevent their

phone from using a null cipher when making a connection with a cell tower [81]. When the null cipher is used, communications are sent in the clear and not encrypted. Apple has also taken steps to protect users against cell site simulators and announced that in iOS 17, out September 18, iPhones will not connect to insecure 2G mobile towers if they are placed in Lockdown Mode [38]. As the name implies, Lockdown Mode is a setting that locks down several features for people who are concerned about being attacked by mercenary spyware.

9 CONCLUSION AND FUTURE WORK

In this paper, we have presented FBSDetector, an ML-based FBS and MSA detection system from cellular network, which leverages network traces at Layer 3. To train the ML models, we have created FBSAD and MSAD, the *first-ever* large-scale real-world datasets of 6.6 GB combined, containing 751963 packets. Our novel models, designed specially to detect FBSes and MSAs, perform better than any state-of-the-art model and detect FBSes with a high accuracy of 92% and a low false positive rate of 5.96%, and MSAs with 86% accuracy and 7.82% false positive rate. We deploy FBSDetector on an Android app that effectively detects FBSes in all the tested real-world scenarios.

Future work: In the future, we will port FBSDetector to 5G and focus on detecting FBSes within the emerging Open Radio Access Network (ORAN) environment, employing advanced machine learning algorithms through xApps. We will also incorporate federated learning in UE clusters at the network edge to detect FBSes and MSAs.

ACKNOWLEDGEMENTS

This work is supported by NSF Grant No. 2112471. We thank the POWDER team for their support in utilizing the platform.

REFERENCES

- [1] HOW MANY PEOPLE HAVE SMARTPHONES IN 2023?. <https://www.oberlo.com/statistics/how-many-people-have-smartphones>.
- [2] Forecast number of mobile devices worldwide from 2020 to 2025 (in billions)*. <https://www.statista.com/statistics/245501/multiple-mobile-device-ownership-worldwide/>.
- [3] Mitziu Echeverria, Zeeshan Ahmed, Bincheng Wang, M. Fareed Arif, Syed Rafiul Hussain, and Omar Chowdhury. PHOENIX: device-centric cellular network protocol monitoring using runtime verification. In *28th Annual Network and Distributed System Security Symposium, NDSS 2021, virtually, February 21-25, 2021*. The Internet Society, 2021.
- [4] Syed Rafiul Hussain, Mitziu Echeverria, Ankush Singla, Omar Chowdhury, and Elisa Bertino. Insecure connection bootstrapping in cellular networks: The root of all evil. In *Proceedings of the 12th Conference on Security and Privacy in Wireless and Mobile Networks, WiSec '19*, page 1–11, New York, NY, USA, 2019. Association for Computing Machinery.
- [5] CheolJun Park, Sangwook Bae, BeomSeok Oh, Jiho Lee, Eunhyu Lee, Insu Yun, and Yongdae Kim. {DoLTest}: In-depth downlink negative testing framework for {LTE} devices. In *31st USENIX Security Symposium (USENIX Security 22)*, pages 1325–1342, 2022.
- [6] Hongil Kim, Jiho Lee, Eunhyu Lee, and Yongdae Kim. Touching the untouchables: Dynamic security analysis of the lte control plane. In *2019 IEEE Symposium on Security and Privacy (SP)*, pages 1153–1168, 2019.
- [7] Syed Rafiul Hussain, Omar Chowdhury, Shagufta Mehnaz, and Elisa Bertino. Liteinspector: A systematic approach for adversarial testing of 4g lte. In *Network and Distributed System Security Symposium*, 2018.
- [8] Altaf Shaik, Jean-Pierre Seifert, Ravishankar Borgaonkar, N. Asokan, and Valterri Niemi. Practical attacks against privacy and availability in 4g/lte mobile communication systems. In *23rd Annual Network and Distributed System Security Symposium, NDSS 2016, San Diego, California, USA, February 21-24, 2016*. The Internet Society, 2016.
- [9] Syed Rafiul Hussain, Mitziu Echeverria, Imtiaz Karim, Omar Chowdhury, and Elisa Bertino. 5greasoner: A property-directed security and privacy analysis framework for 5g cellular network protocol. In *Proceedings of the 2019 ACM SIGSAC Conference on Computer and Communications Security, CCS '19*, page 669–684, New York, NY, USA, 2019. Association for Computing Machinery.
- [10] Syed Rafiul Hussain, Mitziu Echeverria, Omar Chowdhury, Ninghui Li, and Elisa Bertino. Privacy attacks to the 4g and 5g cellular paging protocols using side channel information. *Proceedings 2019 Network and Distributed System Security Symposium*, 2019.
- [11] Simon Erni, Martin Kotuliak, Patrick Leu, Marc Roeschlin, and Srđjan Capkun. Adaptover: adaptive overshadowing attacks in cellular networks. In *Proceedings of the 28th Annual International Conference on Mobile Computing And Networking*, pages 743–755, 2022.
- [12] DHS confirms it has detected evidence of mobile snooping devices around DC. <https://www.cnn.com/2018/04/03/politics/dhs-stingrays-washington-dc/index.html>.
- [13] Gang Of Drivers Caught Using Stingrays To Send Fake Links And Steal Cash. <https://thainewsroom.com/2023/05/25/gang-of-drivers-caught-using-stingrays>.
- [14] Merlin Chlosta, David Rupprecht, Christina Pöpper, and Thorsten Holz. 5g sucicatchers: Still catching them all? In *Proceedings of the 14th ACM Conference on Security and Privacy in Wireless and Mobile Networks*, pages 359–364, 2021.
- [15] Ankush Singla, Syed Rafiul Hussain, Omar Chowdhury, Elisa Bertino, and Ninghui Li. Protecting the 4g and 5g cellular paging protocols against security and privacy attacks. *Proceedings on Privacy Enhancing Technologies*, 2020:126 – 142, 2020.
- [16] Ankush Singla, Rouzbeh Behnia, Syed Rafiul Hussain, Attila Yavuz, and Elisa Bertino. Look before you leap: Secure connection bootstrapping for 5g networks to defend against fake base-stations. In *Proceedings of the 2021 ACM Asia Conference on Computer and Communications Security, ASIA CCS '21*, page 501–515, New York, NY, USA, 2021. Association for Computing Machinery.
- [17] 3GPP TS 33.809 Study on 5G security enhancements against False Base Stations (FBS): Certificate based solution for Protecting System Information Messages with Digital Signature in an NPN. https://www.3gpp.org/ftp/TSG_SA/WG3_Security/TSGS3_100Bis-e/Docs/S3-202717.zip.
- [18] Gabriel K. Gegenhuber, Wilfried Mayer, Edgar R. Weippl, and Adrian Dabrowski. Mobileatlas: Geographically decoupled measurements in cellular networks for security and privacy research. In Joseph A. Calandrino and Carmela Troncoso, editors, *32nd USENIX Security Symposium, USENIX Security 2023, Anaheim, CA, USA, August 9-11, 2023*. USENIX Association, 2023.
- [19] Guillem Reus-Muns, Dheryta Jaisinghani, Kunal Sankhe, and Kaushik R. Chowdhury. Trust in 5g open rans through machine learning: Rf fingerprinting on the powder pawr platform. In *GLOBECOM 2020 - 2020 IEEE Global Communications Conference*, pages 1–6, 2020.
- [20] Leyli Karaçay, Zeki Bilgin, Ayşe Bilge Gündüz, Pinar Çomak, Emrah Tomur, Elif Ustundag Soykan, Utku Gülen, and Ferhat Karakoç. A network-based positioning method to locate false base stations. *IEEE Access*, 9:111368–111382, 2021.
- [21] Prajwol Kumar Nakarmi, Mehmet Akif Ersoy, Elif Ustundag Soykan, and Karl Norrman. Murat: Multi-rat false base station detector. *CoRR*, abs/2102.08780, 2021.
- [22] Adrian Dabrowski, Nicola Pianta, Thomas Klepp, Martin Mulazzani, and Edgar Weippl. Imsi-catch me if you can: Imsi-catcher-catchers. In *Proceedings of the 30th Annual Computer Security Applications Conference, ACSAC '14*, page 246–255, New York, NY, USA, 2014. Association for Computing Machinery.
- [23] Cooper Quintin. Detecting fake 4g LTE base stations in real time. USENIX Association, February 2021.
- [24] Arslan Ali and Georg Fischer. Enabling fake base station detection through sample-based higher order noise statistics. In *2019 42nd International Conference on Telecommunications and Signal Processing (TSP)*, pages 695–700, 2019.
- [25] Hamad Alrashed and Riaz Ahmed Shaikh. Imsi catcher detection method for cellular networks. In *2019 2nd International Conference on Computer Applications & Information Security (ICCAIS)*, pages 1–6, 2019.
- [26] Ke-Wen Huang and Huiming Wang. Identifying the fake base station: A location based approach. *IEEE Communications Letters*, 22:1604–1607, 2018.
- [27] Leo Weissbart, Stjepan Picsek, and Lejla Batina. One trace is all it takes: Machine learning-based side-channel attack on eddsa. *Cryptology ePrint Archive, Paper 2019/358*, 2019. <https://eprint.iacr.org/2019/358>.
- [28] Prajwol Kumar Nakarmi, Jakob Sternby, and Ikram Ullah. Applying machine learning on rsrp-based features for false base station detection. In *Proceedings of the 17th International Conference on Availability, Reliability and Security, ARES '22*, New York, NY, USA, 2022. Association for Computing Machinery.
- [29] Zhenhua Li, Weiwei Wang, Christo Wilson, Jian Chen, Chen Qian, Taeho Jung, Lan Zhang, Kebin Liu, Xiangyang Li, and Yunhao Liu. Fbs-radar: Uncovering fake base stations at scale in the wild. *Proceedings 2017 Network and Distributed System Security Symposium*, 2017.
- [30] Darshak. <https://github.com/darshakframework/darshak>.
- [31] The Android-IMSI-Catcher-Detector (short: AIMSICD). <http://www.tea-after-twelve.com/about-us/our-authors/aimsicd>.
- [32] Alessandro Lotto, Vaibhav Singh, Bhaskar Ramasubramanian, Alessandro Brighente, Mauro Conti, and Radha Poovendran. Baron: Base-station authentication through core network for mobility management in 5g networks. In

- Proceedings of the 16th ACM Conference on Security and Privacy in Wireless and Mobile Networks*, WiSec '23, page 133–144, New York, NY, USA, 2023. Association for Computing Machinery.
- [33] SnoopSnitch. https://play.google.com/store/apps/details?id=de.srlabs.snoopsnitch&hl=en_US&gl=US.
- [34] OVERWATCH IMSI CATCHER DETECTION SERVICES. <https://comsec-llc-adds-overwatch>.
- [35] SeaGlass: City-Wide IMSI-Catcher Detection. <https://news.ycombinator.com/item?id=27173717>.
- [36] Zhaowei Tan, Jinghao Zhao, Boyan Ding, and Songwu Lu. CellDAM: User-Space, rootless detection and mitigation for 5g data plane. In *20th USENIX Symposium on Networked Systems Design and Implementation (NSDI 23)*, pages 1601–1619, Boston, MA, April 2023. USENIX Association.
- [37] Junqing Zhang, Guanxiong Shen, Walid Saad, and Kaushik Chowdhury. Radio frequency fingerprint identification for device authentication in the internet of things. *IEEE Communications Magazine*, pages 1–7, 2023.
- [38] Apple and Google Are Introducing New Ways to Defeat Cell Site Simulators, But Is it Enough?. <https://www.eff.org/deeplinks/2023/09/apple-and-google-are-introducing-new-ways-defeat-cell-site-simulators-it-enough>.
- [39] Non-Access-Stratum (NAS) protocol for Evolved Packet System (EPS); Stage 3. <https://portal.3gpp.org/desktopmodules/Specifications/SpecificationDetails.aspx?specificationid=1072>.
- [40] Evolved Universal Terrestrial Radio Access (E-UTRA); Radio Resource Control (RRC); Protocol specification. <https://portal.3gpp.org/desktopmodules/Specifications/SpecificationDetails.aspx?specificationid=2440>.
- [41] Joe Breen, Andrew Buffmire, Jonathon Duerig, Kevin Dutt, Eric Eide, Mike Hibler, David Johnson, Sneha Kumar Kasera, Earl Lewis, Dustin Maas, Alex Orange, Neal Patwari, Daniel Reading, Robert Ricci, David Schurig, Leigh B. Stoller, Jacobus Van der Merwe, Kirk Webb, and Gary Wong. Powder: Platform for open wireless data-driven experimental research. In *Proceedings of the 14th International Workshop on Wireless Network Testbeds, Experimental Evaluation and Characterization, WiNTECH'20*, page 17–24, New York, NY, USA, 2020. Association for Computing Machinery.
- [42] Sergei Chuprov, Leon Reznik, Antoun Obied, and Srujan Shetty. How degrading network conditions influence machine learning end systems performance? In *IEEE INFOCOM 2022 - IEEE Conference on Computer Communications Workshops (INFOCOM WKSHPs)*, pages 1–6, 2022.
- [43] David Johnson, Dustin Maas, and Jacobus Van Der Merwe. Nexran: Closed-loop ran slicing in powder -a top-to-bottom open-source open-ran use case. In *Proceedings of the 15th ACM Workshop on Wireless Network Testbeds, Experimental Evaluation & Characterization, WiNTECH'21*, page 17–23, New York, NY, USA, 2021. Association for Computing Machinery.
- [44] Jose Monterroso, Jacobus Van der Merwe, Kirk Webb, and Gary Wong. Towards using the powder platform for rf propagation validation. In *IEEE INFOCOM 2021 - IEEE Conference on Computer Communications Workshops (INFOCOM WKSHPs)*, pages 1–6, 2021.
- [45] Kirk Webb, Sneha Kumar Kasera, Neal Patwari, and Jacobus Van der Merwe. Wimatch: Wireless resource matchmaking. In *IEEE INFOCOM 2021 - IEEE Conference on Computer Communications Workshops (INFOCOM WKSHPs)*, pages 1–6, 2021.
- [46] Zhenghao Zhang. Zcnet: Achieving high capacity in low power wide area networks. In *2020 IEEE 17th International Conference on Mobile Ad Hoc and Sensor Systems (MASS)*, pages 702–710, 2020.
- [47] Martin Kotuliak, Simon Erni, Patrick Leu, Marc Röschlin, and Srdjan Čapkun. {LTrack}: Stealthy tracking of mobile phones in {LTE}. In *31st USENIX Security Symposium (USENIX Security 22)*, pages 1291–1306, 2022.
- [48] 5G - 4G-5G Subscribers March 2022 - Quarterly update. <https://gsacom.com/paper/4g-5g-subscribers-march-2022-quarterly-update/>.
- [49] Mobile subscriptions outlook. <https://www.ericsson.com/en/reports-and-papers/mobility-report/dataforecasts/mobile-subscriptions-outlook>.
- [50] Tracking the 4G Decade. <https://blog.telegeography.com/tracking-the-4g-decade>.
- [51] The Mobile Economy 2023. <https://www.gsma.com/mobileeconomy/wp-content/uploads/2023/03/270223-The-Mobile-Economy-2023.pdf>.
- [52] Number of LTE subscriptions worldwide from 2018 to 2023 (in billions)*. <https://www.statista.com/statistics/206615>.
- [53] Qinli Zhang, Liangdong Qu, and Zhaowen Li. Attribute reduction based on d-s evidence theory in a hybrid information system. *International Journal of Approximate Reasoning*, 148:202–234, 2022.
- [54] Yongchuan Tang, Xu Zhang, Ying Zhou, Yubo Huang, and Deyun Zhou. A new correlation belief function in dempster-shafer evidence theory and its application in classification. *Scientific Reports*, 13(1):7609, May 2023.
- [55] Bedran Karakoc, Nils Fürste, David Rupperecht, and Katharina Kohls. Never let me down again: Bidding-down attacks and mitigations in 5g and 4g. 2023.
- [56] Dempster-Shafer theory. https://en.wikipedia.org/wiki/Dempster%E2%80%93Shafer_theory.
- [57] Open5GS. <https://github.com/open5gs/open5gs>.
- [58] srsRAN. <https://github.com/srsran/srsRAN>.
- [59] tshark. <https://www.wireshark.org/docs/man-pages/tshark.html>.
- [60] Yuanjie Li, Chunyi Peng, Zengwen Yuan, Jiayao Li, Haotian Deng, and Tao Wang. Mobileinsight: Extracting and analyzing cellular network information on smartphones. In *Proceedings of the 22nd Annual International Conference on Mobile Computing and Networking, MobiCom '16*, page 202–215, New York, NY, USA, 2016. Association for Computing Machinery.
- [61] tensorflow-lite. https://www.tensorflow.org/lite/guide/inference?utm_campaign=Thoughts%20on%20HCL%20and%20Applied%20AI%20&utm_medium=email&utm_source=Revue%20newsletter.
- [62] flutter. <https://docs.flutter.dev/>.
- [63] USRP B210 SDR Kit - Dual Channel Transceiver (70 MHz - 6GHz) - Ettus Research. <https://www.ettus.com/all-products/ub210-kit/>.
- [64] Adrian Dabrowski, Georg Petzl, and Edgar R. Weippl. The messenger shoots back: Network operator based imsi catcher detection. In *International Symposium on Recent Advances in Intrusion Detection*, 2016.
- [65] Tuan Dinh Hoang, CheolJun Park, Mincheol Son, Taekkyung Oh, Sangwook Bae, Junho Ahn, Beomseok Oh, and Yongdae Kim. Ltesniffer: An open-source lte downlink/uplink eavesdropper. 2023.
- [66] Hojoon Yang, Sangwook Bae, Mincheol Son, Hongil Kim, Song Min Kim, and Yongdae Kim. Hiding in plain signal: Physical signal overshadowing attack on {LTE}. In *28th USENIX Security Symposium (USENIX Security 19)*, pages 55–72, 2019.
- [67] David Rupperecht, Katharina Kohls, Thorsten Holz, and Christina Pöpper. Call me maybe: Eavesdropping encrypted lte calls with revolte. In *Proceedings of the 29th USENIX Conference on Security Symposium, SEC'20*, USA, 2020. USENIX Association.
- [68] David Rupperecht, Katharina Kohls, Thorsten Holz, and Christina Pöpper. Breaking lte on layer two. In *2019 IEEE Symposium on Security and Privacy (SP)*, pages 1121–1136. IEEE, 2019.
- [69] Evangelos Bitsikas and Christina Pöpper. Don't hand it over: Vulnerabilities in the handover procedure of cellular telecommunications. In *Annual Computer Security Applications Conference, ACSAC '21*, page 900–915, New York, NY, USA, 2021. Association for Computing Machinery.
- [70] Daniel Klischies, Moritz Schloegel, Tobias Scharnowski, Mikhail Bogodukhov, David Rupperecht, and Veelasha Moonsamy. Instructions unclear: Undefined behaviour in cellular network specifications. In *32nd USENIX Security Symposium (USENIX Security 23)*, pages 3475–3492, Anaheim, CA, August 2023. USENIX Association.
- [71] David Rupperecht, Katharina Kohls, Thorsten Holz, and Christina Pöpper. Imp4gt: Impersonation attacks in 4g networks. In *ISOC Network and Distributed System Security Symposium (NDSS)*. ISOC, February 2020.
- [72] Yi Chen, Yepeng Yao, XiaoFeng Wang, Dandan Xu, Chang Yue, Xiaozhong Liu, Kai Chen, Haixu Tang, and Baoxu Liu. Bookworm game: Automatic discovery of lte vulnerabilities through documentation analysis. In *2021 IEEE Symposium on Security and Privacy (SP)*, pages 1197–1214, 2021.
- [73] Yi Chen, Di Tang, Yepeng Yao, Mingming Zha, XiaoFeng Wang, Xiaozhong Liu, Haixu Tang, and Baoxu Liu. Sherlock on specs: Building LTE conformance tests through automated reasoning. In *32nd USENIX Security Symposium (USENIX Security 23)*, pages 3529–3545, Anaheim, CA, August 2023. USENIX Association.
- [74] Yi Chen, Di Tang, Yepeng Yao, Mingming Zha, XiaoFeng Wang, Xiaozhong Liu, Haixu Tang, and Dongfang Zhao. Seeing the forest for the trees: Understanding security hazards in the {3GPP} ecosystem through intelligent analysis on change requests. In *31st USENIX Security Symposium (USENIX Security 22)*, pages 17–34, 2022.
- [75] Altaf Shaik, Ravishankar Borgaonkar, Shinjo Park, and Jean-Pierre Seifert. On the impact of rogue base stations in 4g/lte self organizing networks. In *Proceedings of the 11th ACM Conference on Security & Privacy in Wireless and Mobile Networks, WiSec '18*, page 75–86, New York, NY, USA, 2018. Association for Computing Machinery.
- [76] Ravishankar Borgaonkar, Lucca Hirschi, Shinjo Park, and Altaf Shaik. New privacy threat on 3g, 4g, and upcoming 5g aka protocols. *Proceedings on Privacy Enhancing Technologies*, 2019:108 – 127, 2019.
- [77] Alexander J Ross and Bradley Reaves. Towards simultaneous attacks on multiple cellular networks. In *2023 IEEE Security and Privacy Workshops (SPW)*, pages 394–405. IEEE, 2023.
- [78] Evangelos Bitsikas and Christina Pöpper. You have been warned: Abusing 5g's warning and emergency systems. In *Proceedings of the 38th Annual Computer Security Applications Conference*, pages 561–575, 2022.
- [79] Intiaz Karim, Syed Rafiul Hussain, and Elisa Bertino. Prochecker: An automated security and privacy analysis framework for 4g lte protocol implementations. In *2021 IEEE 41st International Conference on Distributed Computing Systems (ICDCS)*, pages 773–785, 2021.
- [80] Syed Rafiul Hussain, Intiaz Karim, Abdullah Al Ishtiaq, Omar Chowdhury, and Elisa Bertino. Noncompliance as deviant behavior: An automated black-box noncompliance checker for 4g lte cellular devices. In *Proceedings of the 2021 ACM SIGSAC Conference on Computer and Communications Security, CCS '21*, page 1082–1099, New York, NY, USA, 2021. Association for Computing Machinery.

| Exp No. | Exp Description |
|----------------|--|
| Exp 1, 2 | Fake handover initiation by FBS |
| Exp 3, 10 | No fake base station, no handover |
| Exp 4 | No fake base station, handover tried |
| Exp 5-7, 17-19 | No fake base station, multiple benign handovers |
| Exp 8-9, 11-16 | Fake base station, fake handover attempted and recovered |

Table 9: FBS Experiment Description

| Exp No. | Number of Packets | | | | | |
|---------|-------------------|------------|-------------|---------------|-------------|---------------|
| | NAS | | | RRC | | |
| | Benign | Malicious | Total | Benign | Malicious | Total |
| Exp1 | 33 | 43 | 76 | 2596 | 59 | 2655 |
| Exp2 | 39 | 63 | 102 | 17099 | 25 | 17124 |
| Exp3 | 49 | 0 | 49 | 10197 | 0 | 10197 |
| Exp4 | 5 | 0 | 5 | 47 | 0 | 47 |
| Exp5 | 61 | 0 | 61 | 3367 | 0 | 3367 |
| Exp6 | 66 | 0 | 66 | 2189 | 0 | 2189 |
| Exp7 | 73 | 0 | 73 | 4571 | 0 | 4571 |
| Exp8 | 21 | 42 | 63 | 6088 | 137 | 6225 |
| Exp9 | 13 | 81 | 94 | 5084 | 114 | 5198 |
| Exp10 | 27 | 0 | 27 | 2696 | 0 | 2696 |
| Exp11 | 74 | 101 | 175 | 9332 | 209 | 9541 |
| Exp12 | 65 | 43 | 108 | 89874 | 133 | 90007 |
| Exp13 | 73 | 198 | 271 | 12251 | 275 | 12526 |
| Exp14 | 32 | 48 | 80 | 14569 | 327 | 14896 |
| Exp15 | 62 | 94 | 156 | 10826 | 243 | 11069 |
| Exp16 | 37 | 42 | 79 | 64568 | 96 | 64664 |
| Exp17 | 128 | 0 | 128 | 57202 | 0 | 57202 |
| Exp18 | 27 | 0 | 27 | 24605 | 0 | 24605 |
| Exp19 | 22 | 0 | 22 | 1034 | 0 | 1034 |
| | 907 | 755 | 1662 | 338195 | 1618 | 339813 |

Table 10: Number of packets of each layer in FBSAD

| Packet Name | Benign | Malicious | Total |
|------------------------------|------------|------------|-------------|
| Attach accept | 103 | 1 | 104 |
| Attach complete | 103 | 1 | 104 |
| Attach request | 105 | 173 | 278 |
| Authentication failure | 1 | 172 | 173 |
| Authentication reject | 3 | 0 | 3 |
| Authentication request | 72 | 172 | 244 |
| Authentication response | 71 | 0 | 71 |
| Detach request | 17 | 1 | 18 |
| EMM information | 103 | 1 | 104 |
| Identity request | 44 | 98 | 142 |
| Identity response | 44 | 98 | 142 |
| Security mode command | 71 | 0 | 71 |
| Security mode complete | 71 | 0 | 71 |
| Service reject | 1 | 0 | 1 |
| Tracking area update accept | 9 | 0 | 9 |
| Tracking area update reject | 10 | 9 | 19 |
| Tracking area update request | 60 | 26 | 86 |
| | 888 | 752 | 1640 |

Table 11: NAS Layer Packet Distribution in FBSAD

[81] Android 14 introduces first-of-its-kind cellular connectivity security features. <https://security.googleblog.com/2023/08/android-14-introduces-first-of-its-kind.html>.

A DATASET CONSTRUCTION

A.1 FBS Dataset - FBSAD

The description of different experiments for FBS data generation is given in Table 9. The detailed distributions of the packets are shown in Table 10. The distribution of NAS and RRC layer packets in FBSAD are shown in Table 11 and 12 respectively.

| Packet Name | Benign | Malicious | Total |
|-------------------------------------|------------|------------|------------|
| dlInformationTransfer | 95 | 51 | 146 |
| ulInformationTransfer | 90 | 50 | 140 |
| rrcConnectionRequest | 59 | 35 | 94 |
| rrcConnectionSetup | 59 | 35 | 94 |
| rrcConnectionSetupComplete | 59 | 35 | 94 |
| rrcConnectionRelease | 55 | 36 | 91 |
| systemInformationBlockType1 | 32 | 30 | 62 |
| systemInformation | 32 | 30 | 62 |
| rrcConnectionReconfiguration | 32 | 0 | 32 |
| ueCapabilityInformation | 32 | 0 | 32 |
| ueCapabilityEnquiry | 32 | 0 | 32 |
| securityModeComplete | 32 | 0 | 32 |
| securityModeCommand | 32 | 0 | 32 |
| paging | 5 | 1 | 6 |
| rrcConnectionReestablishmentRequest | 4 | 0 | 4 |
| ueInformationRequest-r9 | 3 | 0 | 3 |
| ueInformationResponse-r9 | 3 | 0 | 3 |
| rrcConnectionReestablishmentReject | 2 | 0 | 2 |
| rrcConnectionReestablishment | 1 | 0 | 1 |
| | 659 | 303 | 962 |

Table 12: RRC Layer Packet Distribution in FBSAD

| Packet Name | Benign | Energy Depletion Attack | NAS Counter Desync Attack | Numb Attack | Paging Channel Hijacking Attack | Total |
|------------------------------|------------|-------------------------|---------------------------|-------------|---------------------------------|-------------|
| Attach accept | 90 | 0 | 0 | 0 | 0 | 90 |
| Attach complete | 90 | 0 | 0 | 0 | 0 | 90 |
| Attach request | 84 | 108 | 0 | 128 | 28 | 348 |
| Authentication reject | 0 | 0 | 0 | 8 | 0 | 8 |
| Authentication request | 74 | 60 | 0 | 0 | 0 | 134 |
| Authentication response | 74 | 60 | 0 | 0 | 0 | 134 |
| Detach request | 27 | 0 | 0 | 0 | 0 | 27 |
| EMM information | 90 | 0 | 0 | 0 | 0 | 90 |
| Identity request | 48 | 24 | 0 | 0 | 8 | 80 |
| Identity response | 48 | 24 | 0 | 0 | 8 | 80 |
| Security mode command | 74 | 60 | 245 | 0 | 0 | 379 |
| Security mode complete | 74 | 60 | 0 | 0 | 0 | 134 |
| Security mode reject | 0 | 0 | 245 | 0 | 0 | 245 |
| Service reject | 1 | 0 | 0 | 0 | 0 | 1 |
| Tracking area update accept | 5 | 0 | 0 | 0 | 0 | 5 |
| Tracking area update reject | 11 | 12 | 0 | 0 | 4 | 27 |
| Tracking area update request | 43 | 12 | 1 | 8 | 4 | 68 |
| | 833 | 420 | 491 | 144 | 52 | 1940 |

Table 13: NAS layer Packet Distribution in MSAD

| Packet Name | Benign | Energy Depletion Attack | NAS Counter Desync Attack | Numb Attack | Paging Channel Hijacking Attack | Total |
|------------------------------|------------|-------------------------|---------------------------|-------------|---------------------------------|------------|
| dlInformationTransfer | 30 | 20 | 17 | 4 | 4 | 75 |
| ulInformationTransfer | 30 | 24 | 11 | 0 | 5 | 70 |
| systemInformationBlockType1 | 8 | 13 | 4 | 6 | 5 | 36 |
| rrcConnectionRequest | 13 | 9 | 3 | 1 | 4 | 30 |
| rrcConnectionSetup | 13 | 9 | 3 | 1 | 4 | 30 |
| rrcConnectionSetupComplete | 12 | 9 | 3 | 1 | 4 | 29 |
| rrcConnectionRelease | 8 | 9 | 3 | 0 | 4 | 24 |
| systemInformation | 8 | 7 | 2 | 1 | 2 | 20 |
| rrcConnectionReconfiguration | 10 | 0 | 0 | 0 | 0 | 10 |
| ueCapabilityInformation | 9 | 0 | 0 | 0 | 0 | 9 |
| securityModeCommand | 9 | 0 | 0 | 0 | 0 | 9 |
| ueCapabilityEnquiry | 9 | 0 | 0 | 0 | 0 | 9 |
| securityModeComplete | 9 | 0 | 0 | 0 | 0 | 9 |
| ueInformationRequest-r9 | 2 | 0 | 0 | 0 | 0 | 2 |
| ueInformationResponse-r9 | 2 | 0 | 0 | 0 | 0 | 2 |
| paging | 1 | 0 | 0 | 0 | 0 | 1 |
| | 173 | 100 | 46 | 14 | 32 | 365 |

Table 14: RRC Layer Packet Distribution in MSAD

A.2 MSA Dataset - MSAD

The detailed distribution of the packets in MSAD is shown in Table 15. The distribution of NAS and RRC layer packets in MSAD are shown in Table 13 and 14 respectively.

| Attack Name | Exp No. | Number of Packets | |
|---------------------------------|---------|-------------------|--------|
| | | NAS | RRC |
| Detach Downgrade Attack | exp-1 | 49 | 1469 |
| | exp-2 | 22 | 830 |
| | exp-3 | 16 | 81 |
| | exp-4 | 16 | 78 |
| | exp-5 | 16 | 86 |
| | exp-6 | 21 | 124 |
| Incarceration Attack | exp-1 | 66 | 171976 |
| | exp-2 | 24 | 109 |
| | exp-3 | 60 | 20081 |
| | exp-4 | 24 | 1169 |
| | exp-5 | 24 | 4079 |
| | exp-6 | 24 | 9067 |
| Stealthy Kickoff Attack | exp-1 | 21 | 82 |
| | exp-2 | 33 | 6888 |
| | exp-3 | 25 | 90 |
| | exp-4 | 25 | 90 |
| | exp-5 | 25 | 91 |
| | exp-6 | 25 | 89 |
| Panic Attack | exp-1 | 17 | 37 |
| | exp-2 | 31 | 1013 |
| | exp-3 | 33 | 87 |
| | exp-4 | 31 | 3847 |
| | exp-5 | 36 | 350 |
| | exp-6 | 51 | 402 |
| NAS Counter Desync Attack | exp-1 | 1554 | 19783 |
| | exp-2 | 1554 | 148 |
| | exp-3 | 6159 | 1360 |
| | exp-4 | 1554 | 422 |
| | exp-5 | 1554 | 176 |
| | exp-6 | 3081 | 233 |
| Energy Depletion Attack | exp-1 | 80 | 1731 |
| | exp-2 | 37 | 137 |
| | exp-3 | 29 | 589 |
| | exp-4 | 29 | 196 |
| | exp-5 | 29 | 109 |
| | exp-6 | 89 | 4457 |
| | exp-7 | 103 | 4519 |
| | exp-8 | 63 | 3130 |
| | exp-9 | 29 | 91 |
| | exp-10 | 105 | 76476 |
| Paging Channel Hijacking Attack | exp-1 | 21 | 85 |
| | exp-2 | 21 | 83 |
| | exp-3 | 21 | 83 |
| | exp-4 | 21 | 86 |
| | exp-5 | 0 | 20 |
| | exp-6 | 21 | 83 |
| Numb Attack | exp-1 | 24 | 108 |
| | exp-2 | 56 | 18399 |
| | exp-3 | 63 | 30087 |
| | exp-4 | 26 | 4478 |
| | exp-5 | 36 | 12011 |
| | exp-6 | 81 | 506 |

Table 15: Number of packets of each layer of different MSA experiment dataset

B EXPERIMENTAL SETUP

B.1 Training Hardware.

For training the models, we utilized a Lenovo ThinkPad T480 equipped with 32GB of memory and an Intel Core i7-8650U CPU @ 1.90GHz \times 8. The operating system was Ubuntu 22.04.1 LTS (64-bit), running GNOME Version 42.2.

B.2 Model Hyperparameters.

Sequential LSTM. The Sequential-LSTM model consists of an *LSTM* layer with 64 units and a *sigmoid* activation function, configured not to return sequences. The subsequent layer is a dense

layer with a single unit and *sigmoid* activation. For optimization, *stochastic gradient descent (sgd)* was chosen, with a *mean squared error (mse)* loss function. The model’s performance is assessed using *accuracy* as the main metric, complemented by the inclusion of a custom metric, *false positives*, to evaluate its classification capabilities further.

GraphSAGE. The graph model is implemented featuring a single *SAGEConv* layer. The *SAGEConv* layer utilizes 2 attention heads to capture graph-based relationships. The model’s architecture is encapsulated within a *PyTorch* Module, with the forward function defining the flow of information through the single layer. Logarithmic *softmax* is employed for the final layer’s output activation.

Other Graph Models. For the other graph models, we used the same configurations as the *GraphSAGE* model with their own convolutional layer. For example, for the Graph Attention Network, we used *GATConv*, and for the Graph Convolutional Network, we used *GCNConv*.

Other Classification Models. The Random Forest Classifier and the Decision Tree Classifier were configured with a Gini criterion, a maximum depth of 3. The XGBoost Classifier, Support Vector Classifier (SVC), K-Nearest-Neighbors (KNN) Classifier, Gaussian Naive Bayes and Logistic Regression adopted default configurations.

Convolutional Neural Network (CNN). The CNN architecture comprises two *Conv1D* layers with 32 and 64 filters, respectively, followed by a *ReLU* activation function. *MaxPooling1D* layers with a pool size of 2 were inserted after each convolutional layer to downsample the spatial dimensions. A *GlobalAveragePooling1D* layer was then employed to aggregate the spatial information across the entire sequence. Subsequently, two Dense layers were added with 64 units and *ReLU* activation in the first, and a single unit with a *sigmoid* activation in the final layer for classification. The model was compiled using the Adam optimizer, binary cross-entropy loss function, and accuracy as the metric for performance evaluation.

Feedforward Neural Network (FNN). The FNN architecture consists of three Dense layers, with the first two layers containing 64 units each and utilizing the *ReLU* activation function. The final dense layer, with a single unit and a *sigmoid* activation function, is employed for classification. The model was compiled using the Adam optimizer, *binary cross-entropy* as the loss function, and *accuracy* as the metric for assessing its performance.

C POWDER

POWDER (Platform for Open Wireless Data-driven Experimental Research) resolves all these challenges and provides us with a way to generate high-quality, real-world, over-the-air datasets of FBSes with all the real-world scenarios involved, especially mobility. This invaluable resource enables us to develop and test FBS detection algorithms in a realistic environment. POWDER is a highly flexible city-scale scientific instrument that enables research at the forefront of the wireless revolution [41] and is currently deployed in Salt Lake City, Utah. POWDER is a partnership between the University of Utah, Salt Lake City, and other public and private organizations (local, national, and global).

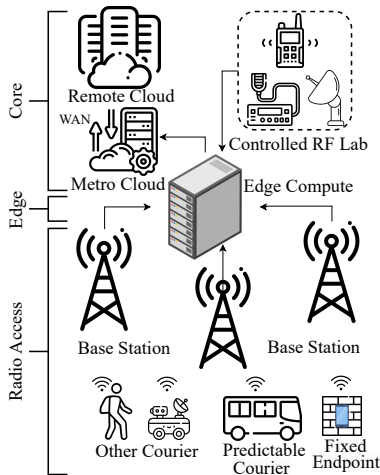


Figure 9: POWDER overview

C.1 Hardware and Mobility

The physical deployment of POWDER encompasses three key components: (1) **Core Component**: This includes the Controlled RF Lab and the Metro Cloud situated on-premise, connected to a remote cloud through a wide area network (WAN). (2) **Edge Component**: This involves edge computing devices to facilitate processing closer to data sources. (3) **Radio Access Component**: Comprising base stations, fixed, and mobile endpoints, this component establishes the fundamental wireless communication infrastructure. The physical deployment offers a variety of configurable “coverage” scenarios, e.g., conventional macro-cell, small-cell (enabled by the campus “dense” deployment), or combinations thereof. Diversity in *mobility* is provided by using mobile couriers that have relatively predictable movement patterns (e.g., buses), less predictable but bounded mobility (e.g., maintenance vehicles), and couriers that are “controllable” (e.g., backpacks/portable endpoints that can be moved by researchers that come on-site). Each deployed node consists of user-programmable software-defined radios (SDRs), off-the-shelf (OTS) radio equipment, RF front-ends, and antennas. An architectural overview of POWDER is given in Figure 9.

C.2 Software and Profiles

In the context of POWDER, profiles refer to configurable sets of parameters that define various aspects of the wireless network environment. These parameters encompass hardware, network configurations, signal propagation characteristics, mobility patterns, interference scenarios, and more. Profiles make it possible to replicate real-world conditions for experimentation, allowing one to create diverse scenarios, including those involving FBSes. Using profiles, one can manipulate the network environment within POWDER’s controlled setting and conduct experiments that closely mirror real-world situations while avoiding legal and regulatory challenges. By creating different profiles, one can effectively create real-world conditions. This capability is a significant advantage, allowing one to conduct comprehensive experiments and analyses within a controlled environment.

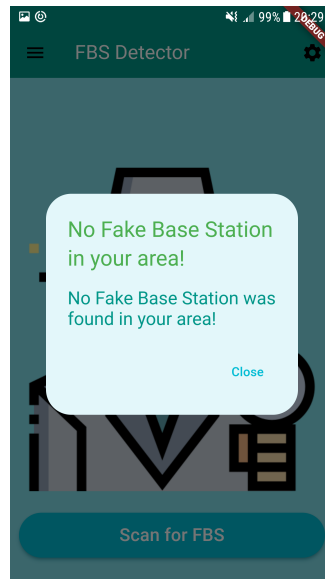
POWDER feedback POWDER makes it possible to replicate real-world conditions for experimentation. One can manipulate the network environment within POWDER’s controlled setting and conduct experiments using POWDER profiles. However, only a limited number of profiles with some fixed sets of parameters are currently available at POWDER. Users can create their profiles according to their requirements. Still, a new user might find it challenging to create a profile because there is not enough documentation and tutorials on creating these profiles. The incorporation of more profiles with diverse scenarios, automation of the profile creation process, and extensive documentation and tutorials will help users utilize POWDER’s capabilities to a great extent.

D MOBILE APP

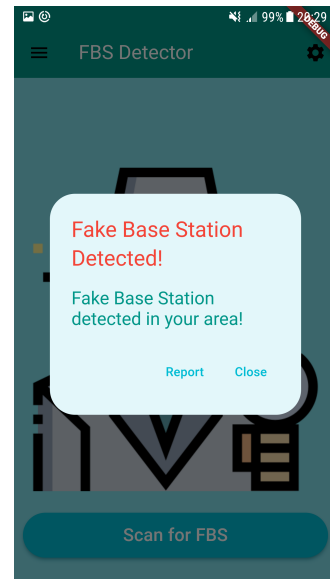
Different components of the FBSDetector Android app are demonstrated in Figure 10.



(a) Homepage of FBS Detector



(b) No Fake Base Station detected



(c) Fake Base Station detected

Figure 10: Android app for FBSDetector